Taylor & Francis Online

Journals | Search | Publish

Access provided by
Kocaeli Universitesi

Login | Register

Home ▶ All Journals ▶ Bioscience ▶ Connective Tissue Research



Connective Tissue Research

Share

Open Select: choose to publish open access

Publishes research on mechanisms and structure-function relationships in the connective tissue extracellular matrix and biological process of tissue repair.

Enter keywords, authors, DOI, etc

This Journal

Advanced search Citation search

Submit | About | Browse | Subscribe

Favorite Export

JCR Year 2024

CONNECTIVE TISSUE RESEARCH

ISSN

0300-8207

EISSN

1607-8438

JCR ABBREVIATION

CONNECT TISSUE RES

ISO ABBREVIATION

Connect. Tissue Res.

Journal information

EDITION

Science Citation Index Expanded (SCIE)

CATEGORY

CELL BIOLOGY

ORTHOPEDICS

LANGUAGES

English

REGION

ENGLAND

1ST ELECTRONIC JCR YEAR

1997

Publisher information

PUBLISHER

TAYLOR & FRANCIS INC

ADDRESS

530 WALNUT STREET, STE 850, PHILADELPHIA, PA 19106

PUBLICATION FREQUENCY

6 issues/year

Journal's performance

Journal Impact Factor

The Journal Impact Factor (JIF) is a journal-level metric calculated from data indexed in the Web of Science Core Collection. It should be used with careful attention to the many factors that influence citation rates, such as the volume of publication and citations characteristics of the subject area and type of journal. The Journal Impact Factor can complement expert opinion and informed peer review. In the case of academic evaluation for tenure, it is inappropriate to use a journal-level metric as a proxy measure for individual researchers, institutions, or articles. Learn more

2024 JOURNAL IMPACT FACTOR

2.1

View calculation

JOURNAL IMPACT FACTOR WITHOUT SELF CITATIONS

2.0

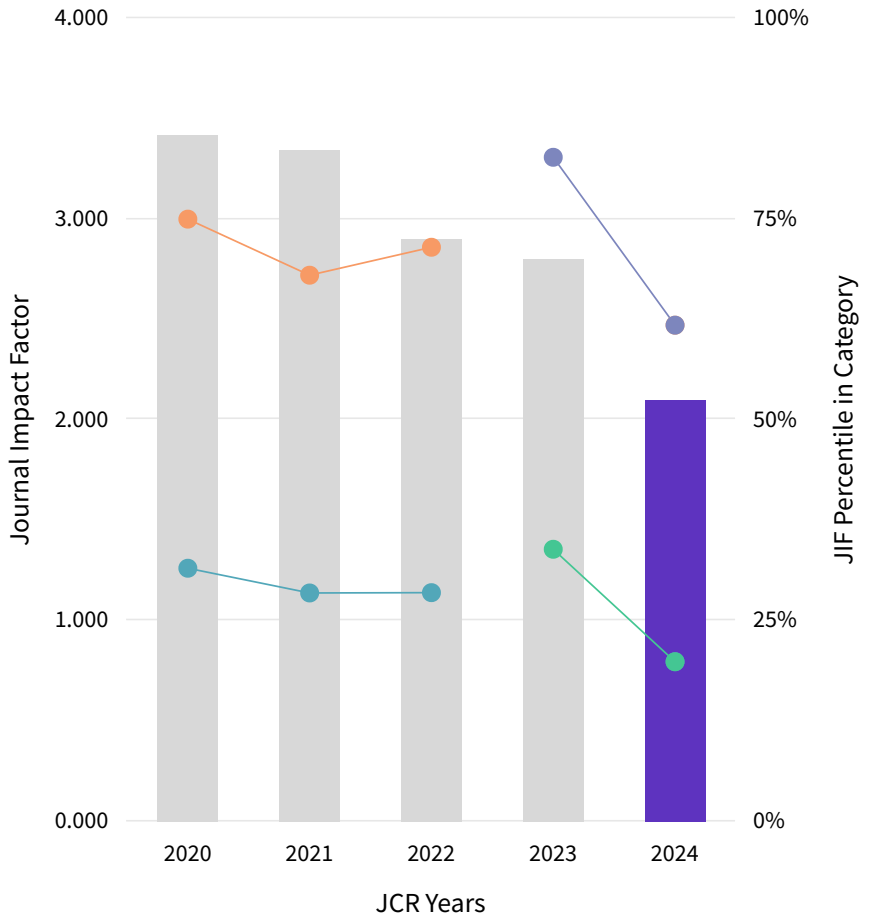
View calculation

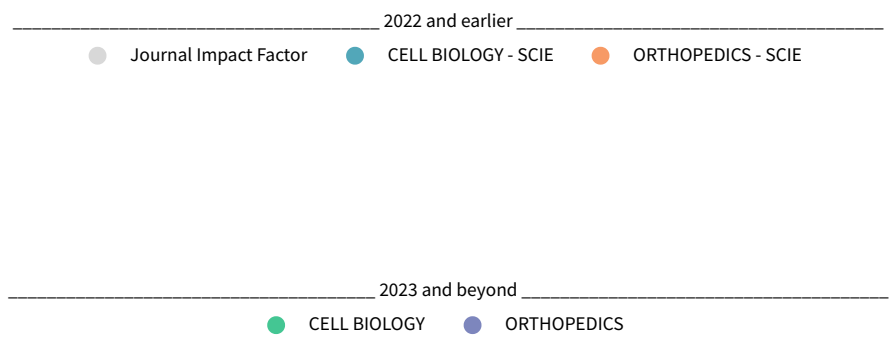
Journal Impact Factor Trend 2024 Export

Journal Impact Factor contributing items Export

Citable items (73) | Citing Sources (119)

TITLE	CITATION COUNT
Proanthocyanidins inhibit the apoptosis and aging of nucleus pulposus cells…	9
Oral mucosa equivalents, prevascularization approaches, and…	8





Role of pro-inflammatory interleukins in osteoarthritis: a narrative review	8
Impact of aging on tendon homeostasis, tendinopathy development, and impair…	7
Collagen misfolding mutations: the contribution of the unfolded protein…	5
Contribution of immune cells to intervertebral disc degeneration and th…	5
Current status and future trends of reconstructing a vascularized tissue-…	5
Extracellular vesicles from human umbilical cord mesenchymal stem cells…	5
Metformin reduces myogenic contracture and myofibrosis induced by rat knee joi…	5
miR-34a-5p facilitates osteogenic differentiation of bone marrow…	5

View All in Web of Science

View all years

Journal Citation Indicator (JCI)

Export

0.74

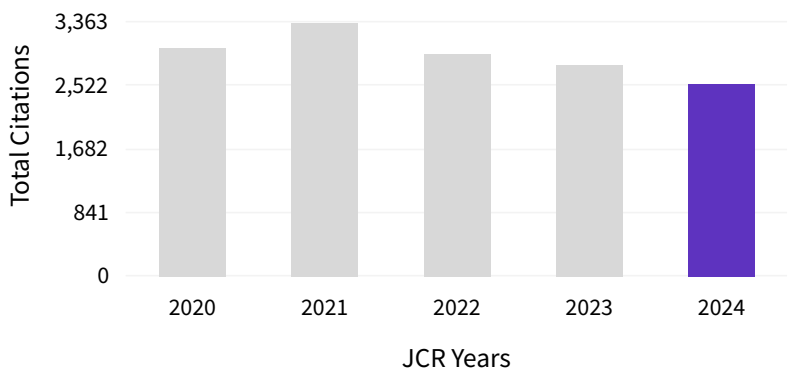
The Journal Citation Indicator (JCI) is the average Category Normalized Citation Impact (CNCI) of citable items (articles & reviews) published by a journal over a recent three year period. The average JCI in a category is 1. Journals with a JCI of 1.5 have 50% more citation impact than the average in that category. It may be used alongside other metrics to help you evaluate journals. Learn more

Total Citations

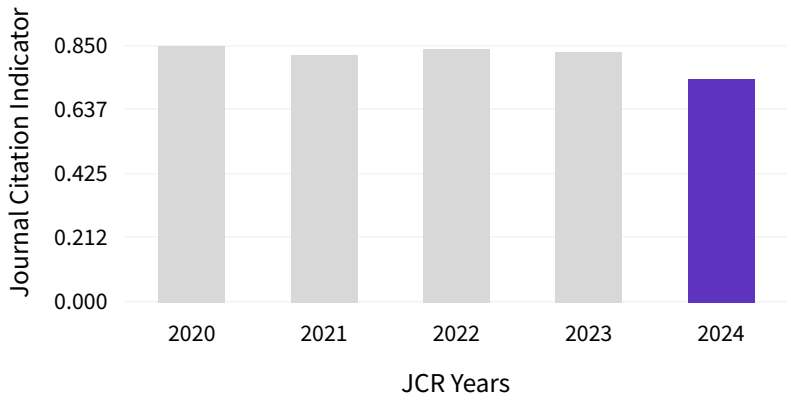
Export

2,556

The total number of times that a journal has been cited by all journals included in the database in the JCR year. Citations to journals listed in JCR are compiled annually from the JCR years combined database, regardless of which JCR edition lists the journal.



15



View all years

View all years

Citation distribution

Export

The Citation Distribution shows the frequency with which items published in the year or two years prior were cited in the JCR data year (i.e., the component of the calculation of the JIF). The graph has similar functionality as the JIF Trend graph, including hover-over data descriptions for each data point, and an interactive legend where each data element's legend can be used as a toggle. You can view Articles, Reviews, or Non-Citable (other) items to the JIF numerator. Learn more

ARTICLE CITATION MEDIAN

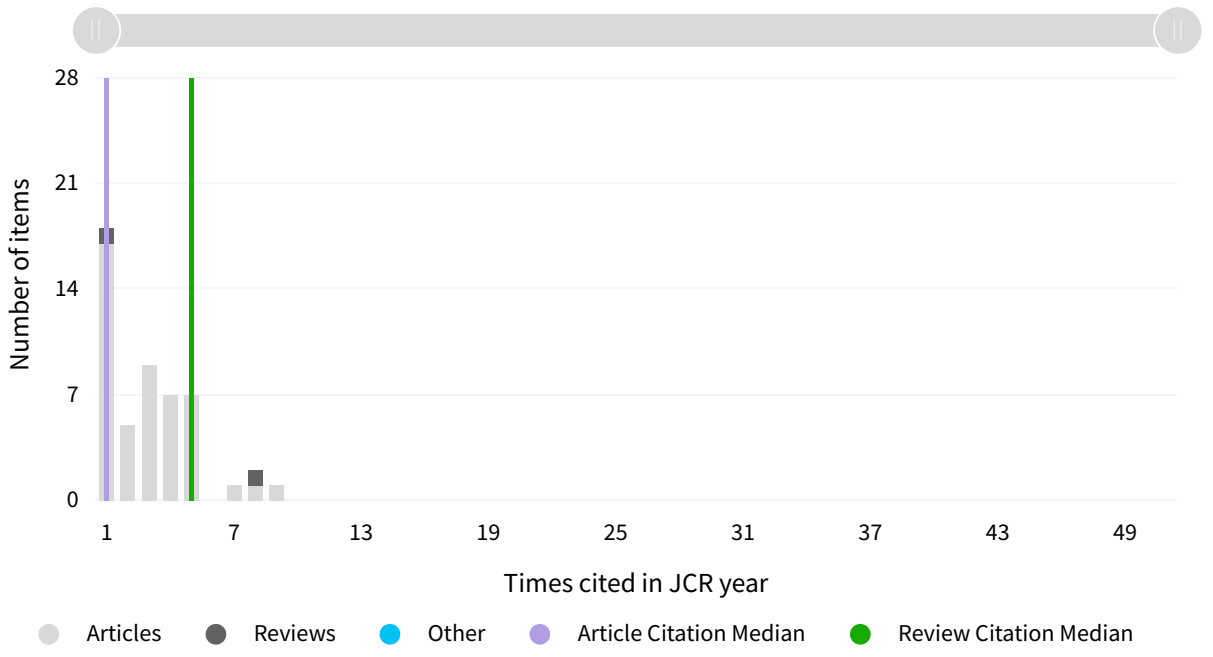
1

REVIEW CITATION MEDIAN

4.5

UNLINKED CITATIONS

5



TIMES CITED

0

ARTICLES

23

REVIEWS

0

OTHER

2

Open Access (OA)

Export

The data included in this tile summarizes the items published in the journal in the JCR data year and in the previous two years. This three-year set of published items is used to provide descriptive analysis of the content and community of the journal. Learn more

Items

TOTAL CITABLE	% OF CITABLE OA
108	7.41%

Citations*

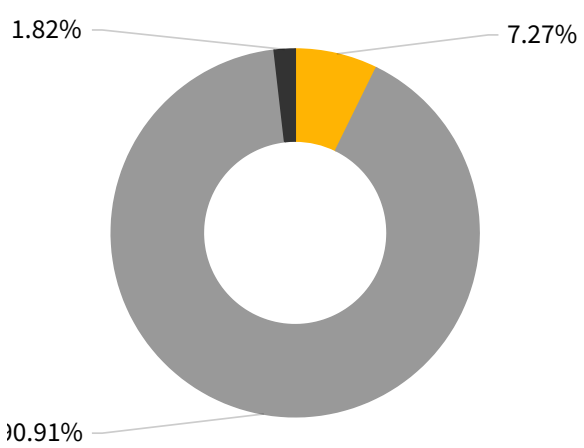
TOTAL CITABLE	% OF CITABLE OA
167	5.99%

15

CITABLE

GOLD OPEN ACCESS
8 / 7.27%

SUBSCRIPTION AND FREE TO READ
100 / 90.91%



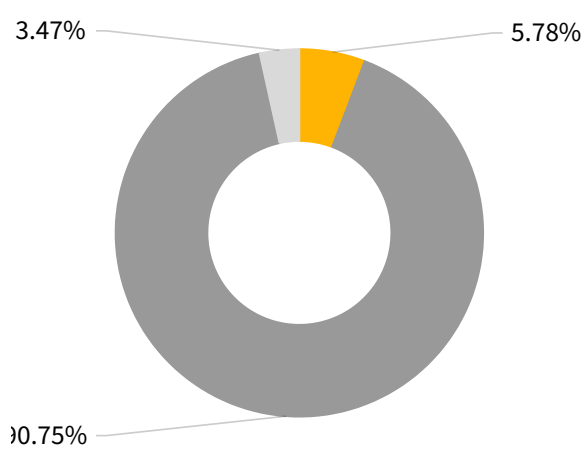
NON-CITABLE

OTHER (NON CITABLE ITEMS)
2 / 1.82%

CITABLE

GOLD OPEN ACCESS
10 / 5.78%

SUBSCRIPTION AND FREE TO READ
157 / 90.75%



NON-CITABLE

OTHER (NON CITABLE ITEMS)
0 / 0.00%

UNLINKED CITATIONS
6 / 3.47%

*Citations in 2024 to items published in [2022 - 2024]

Rank by Journal Impact Factor

Journals within a category are sorted in descending order by Journal Impact Factor (JIF) resulting in the Category Ranking below. A separate rank is shown for each category in which the journal is listed in JCR. Beginning in 2023, ranks are calculated by category.
Learn more

CATEGORY
CELL BIOLOGY

164/204

JCR YEAR	JIF RANK	JIF QUARTILE	JIF PERCENTILE
2024	164/204	Q4	19.9
2023	136/205	Q3	33.9

CATEGORY
ORTHOPEDICS

54/140

JCR YEAR	JIF RANK	JIF QUARTILE	JIF PERCENTILE
2024	54/140	Q2	61.8
2023	24/136	Q1	82.7

Rank by JIF before 2023 for CELL BIOLOGY

EDITION
Science Citation Index Expanded (SCIE)

JCR YEAR	JIF RANK	JIF QUARTILE	JIF PERCENTILE
2022	137/191	Q3	28.5
2021	140/195	Q3	28.46
2020	134/195	Q3	31.54
2019	130/195	Q3	33.59

Rank by JIF before 2023 for ORTHOPEDICS

EDITION
Science Citation Index Expanded (SCIE)

JCR YEAR	JIF RANK	JIF QUARTILE	JIF PERCENTILE
2022	25/86	Q2	71.5
2021	28/86	Q2	68.02
2020	21/82	Q2	75.00
2019	21/82	Q2	75.00

Rank by Journal Citation Indicator (JCI)

15

Journals within a category are sorted in descending order by Journal Citation Indicator (JCI) resulting in the Category Ranking below. A separate rank is shown for each category in which the journal is listed in JCR. Data for the most recent year is presented at the top of the list, with other years shown in reverse chronological order. Learn more

CATEGORY
CELL BIOLOGY
91/204

JCR YEAR	JCI RANK	JCI QUARTILE	JCI PERCENTILE
2024	91/204	Q2	55.64
2023	79/205	Q2	61.71
2022	79/203	Q2	61.33
2021	73/204	Q2	64.46
2020	74/201	Q2	63.43
2019	94/200	Q2	53.25
2018	103/200	Q3	48.75

CATEGORY
ORTHOPEDICS
70/140

JCR YEAR	JCI RANK	JCI QUARTILE	JCI PERCENTILE
2024	70/140	Q2	50.36
2023	52/136	Q2	62.13
2022	48/130	Q2	63.46
2021	45/127	Q2	64.96
2020	40/119	Q2	66.81
2019	47/119	Q2	60.92
2018	52/118	Q2	56.36

Citation network

Cited Half-life

9.5 years

The Cited Half-Life is the median age of the items in this journal that were cited in the JCR year. Half of a journal's cited items were published more recently than the cited half-life.

TOTAL NUMBER OF CITES

2,556

NON SELF-CITATIONS

2,542

SELF-CITATIONS

14

Citing Half-life

7.9 years

The Citing Half-Life is the median age of items in other publications cited by this journal in the JCR year.

TOTAL NUMBER OF CITES

2,049

NON SELF-CITATIONS

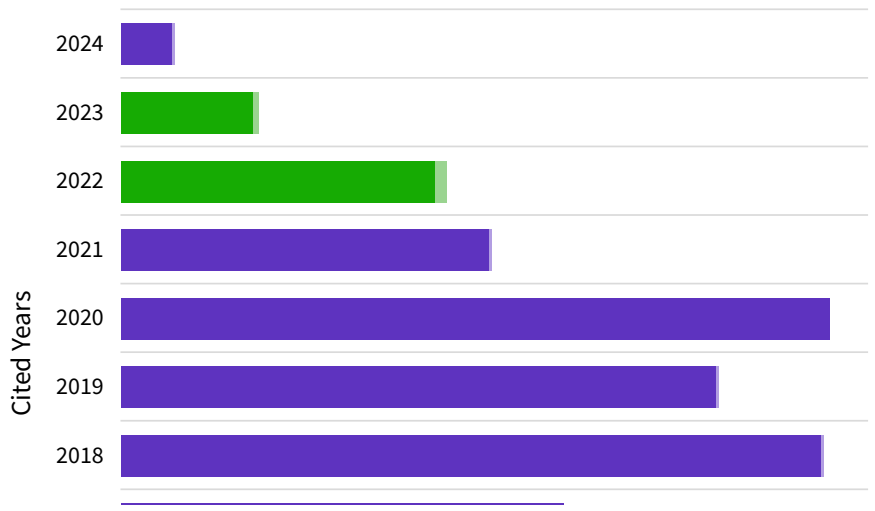
2,035

SELF-CITATIONS

14

Cited Half-life Data | Citing Half-life Data

Export

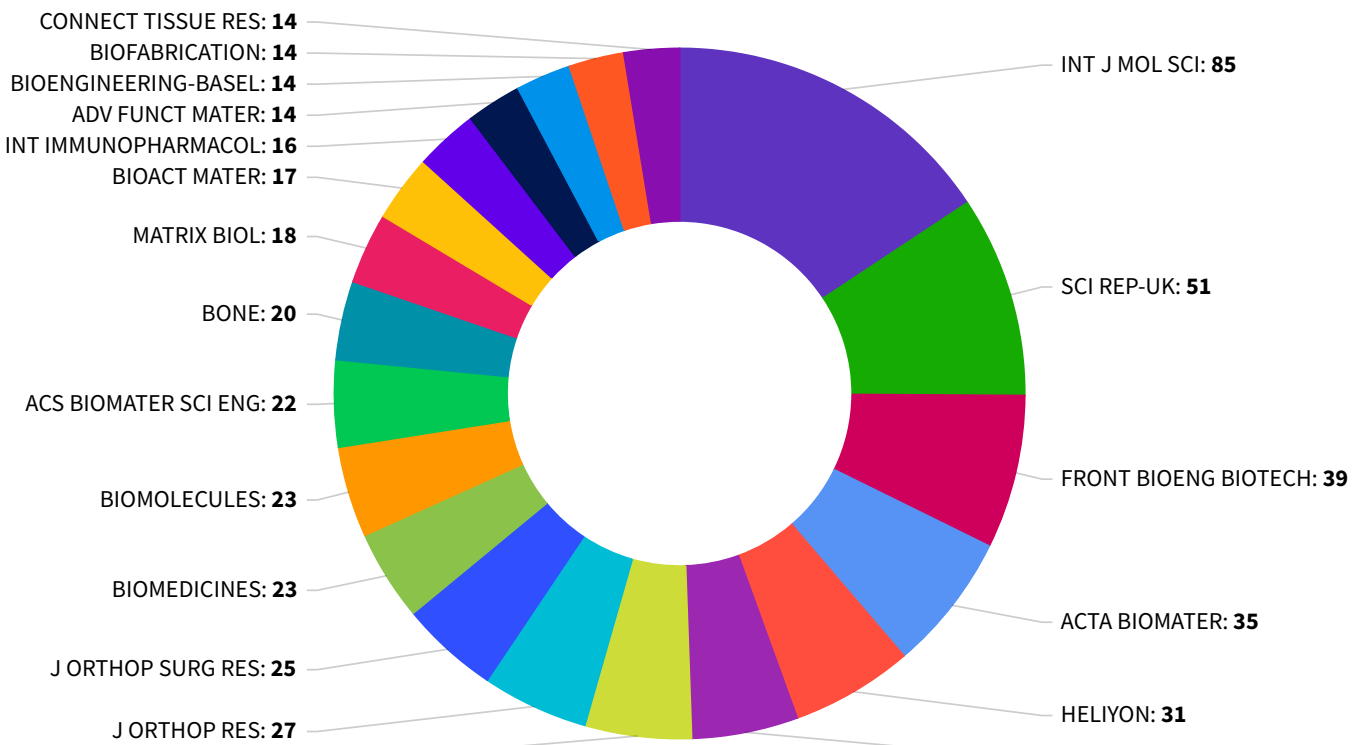


CITED YEAR	# OF CITES FROM 2024	CUMULATIVE %	# OF CITING SOURCES
All years	**2,556 citations**	**100.00%**	**941 sources**
2024	18 citations	0.70%	17 sources
2023	46 citations	2.50%	41 sources
2022	109 citations	6.77%	86 sources
2021	124 citations	11.62%	104 sources
2020	237 citations	20.89%	168 sources
2019	200 citations	28.72%	144 sources
2018	235 citations	37.91%	178 sources

Journal Citation Relationships

Cited Data | Citing Data

Top 20 journals citing CONNECT TISSUE RES by number of citations



Content metrics

Source data

This tile shows the breakdown of document types published by the journal. Citable Items are Articles and Reviews. For the purposes of calculating JIF, a JCR year considers the publications of that journal in the two prior years. Learn more

Average JIF Percentile

Export

The Average Journal Impact Factor Percentile takes the sum of the JIF Percentile rank for each category under consideration, then calculates the average of those values. Learn more

15

35 total citable items

	ARTICLES	REVIEWS	COMBINED(C)	OTHER DOCUMENT TYPES(O)	PERCENTAG
NUMBER IN JCR YEAR 2024 (A)	29	6	35	0	100%
NUMBER OF REFERENCES (B)	1,394	655	2,049	0	100%
RATIO (B/A)	48.1	109.2	58.5	N/A	

ALL CATEGORIES AVERAGE
40.9

ORTHOPEDICS
61.8

CELL BIOLOGY
19.9

Contributions by organizations

Export

Organizations that have contributed the most papers to the journal in the most recent three-year period. Learn more

RANK	ORGANIZATION	COUNT
1	ANHUI MEDICAL UNIVERSITY	4
-	PEKING UNIVERSITY	4
3	CENTRAL SOUTH UNIVERSITY	3
-	HIROSHIMA INTERNATIONAL UNIVERSITY	3
-	NATL CLIN RES CTR ORAL DIS	3
-	QINGDAO UNIVERSITY	3
-	TONGJI UNIVERSITY	3
-	UNIVERSITY OF CALGARY	3

Contributions by country/region

Export

Countries or Regions that have contributed the most papers to the journal in the most recent three-year period. Learn more

RANK	COUNTRY / REGION	COUNT
1	CHINA MAINLAND	51
2	USA	29
3	JAPAN	11
4	CANADA	6
5	FINLAND	3
-	IRAN	3
-	TURKIYE	3
8	ENGLAND	2
-	INDIA	2

Additional metrics

Eigenfactor Score

0.00127

The Eigenfactor Score is a reflection of the density of the network of citations around the journal using 5 years of cited content as cited by the Current Year. It considers both the number of citations and the source of those citations, so that highly cited sources will influence the network more than

Normalized Eigenfactor

0.28517

The Normalized Eigenfactor Score is the Eigenfactor score normalized, by rescaling the total number of journals in the JCR each year, so that the average journal has a score of 1. Journals can then be compared and influence measured by their score relative to 1. Learn more

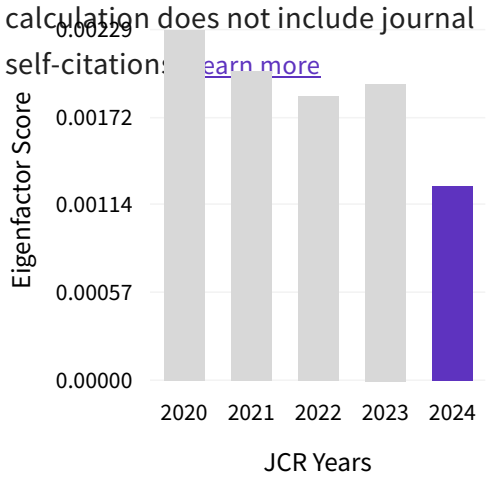
Article influence score

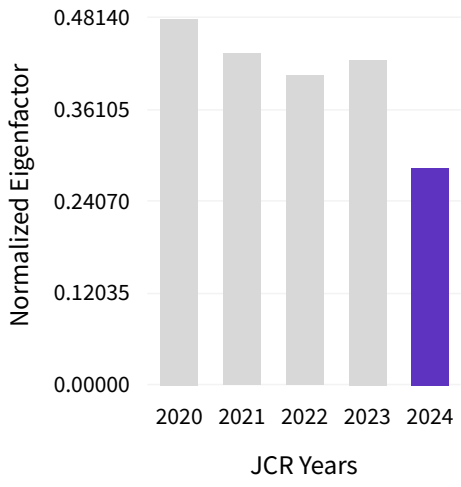
0.595

The Article Influence Score normalizes the Eigenfactor Score according to the cumulative size of the cited journal across the prior five years. The mean Article Influence Score for each article is 1.00. A score greater than 1.00

15

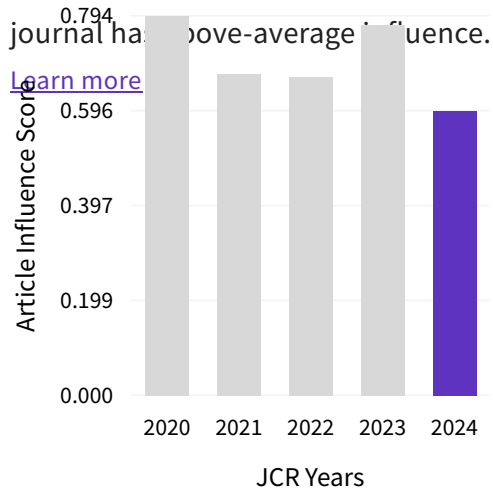
less cited sources. The Eigenfactor calculation does not include journal self-citations. Learn more





indicates that each article in the journal ha[illegible]ove-average influence.

Learn more

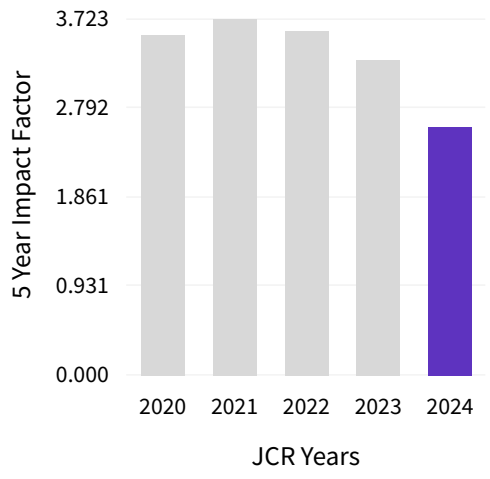


5 Year Impact Factor

2.6

View Calculation

The 5-year Impact Factor is the average number of times articles from the journal published in the past five years have been cited in the JCR year. It is calculated by dividing the number of citations in the JCR year by the total number of articles published in the five previous years. Learn more

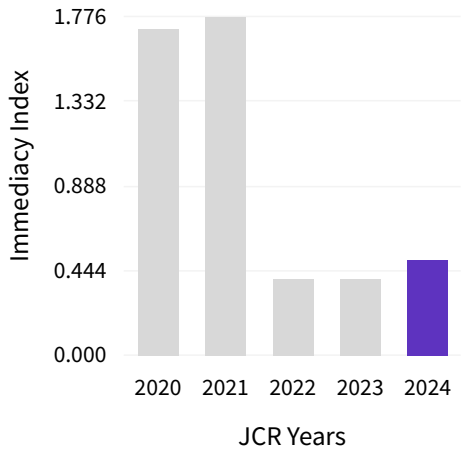


Immediacy Index

0.5

View Calculation

The Immediacy Index is the count of citations in the current year to the journal that reference content in this same year. Journals that have a consistently high Immediacy Index attract citations rapidly. Learn more



© 2025 Clarivate

Legal center

Privacy notice

Cookie policy

Terms of Use

Manage cookie preferences

Copyright notice

Accessibility

Help

Connective Tissue Research

Aims and scope

Journal metrics

Editorial board

Abstracting and indexing

Open access

News and calls for papers

Publication details

Advertising information

Connective Tissue Research

Aims and scope

Journal metrics

Editorial board

Abstracting and indexing

Open access

News and calls for papers

Publication details

Advertising information

Connective Tissue Research

Aims and scope

Journal metrics

Editorial board

Abstracting and indexing

Open access

News and calls for papers

Publication details

Advertising information

Connective Tissue Research

Aims and scope
Journal metrics
Editorial board
Abstracting and indexing
Open access
News and calls for papers
Publication details
Advertising information

Connective Tissue Research

Aims and scope
Journal metrics
Editorial board
Abstracting and indexing
Open access
News and calls for papers
Publication details
Advertising information

Connective Tissue Research

Aims and scope
Journal metrics
Editorial board
Abstracting and indexing
Open access
News and calls for papers
Publication details
Advertising information

Connective Tissue Research

About this journal

Share

Aims and scope

The aim of *Connective Tissue Research* is to present original and significant research in all basic areas of connective tissue and matrix biology.

The journal also provides topical reviews and, on occasion, the proceedings of conferences in areas of special interest at which original work is presented.

Connective Tissue Research

- Biochemistry
- Cell and Molecular Biology

- Biomechanics
- Regenerative Medicine

The interests of the Editorial Board are to understand, mechanistically, the structure function relationships in connective tissue extracellular matrix, and its associated cells, through interpretation of sophisticated experimentation using state-of-the-art technologies that include molecular genetics, imaging, immunology, biomechanics and tissue engineering.

Articles published in the journal present data obtained from such technologies with the ultimate objective of resolving the intricacies of biological processes in health, disease and tissue repair.

The tissues of interest are bone, cartilage, ligament, tendon, muscle, dentin, skin, and teeth, as well as other connective tissue component-rich organs such as skin, the eyes, blood vessels, kidneys and lungs.

Understanding structure and function of extracellular matrix in relation to cellular and biological processes are paramount objectives of the journal in areas of growth, development, aging, tissue remodeling, wound healing, and biomineralization.

The collection of varied but related articles will inform, stimulate and broaden the outlooks of individual specialists interested in current connective tissue research.

Journal metrics

Usage

- **70K** annual downloads/views

Citation metrics

- **2.1 (2024)** Impact Factor
- **Q2** Impact Factor Best Quartile

Speed/acceptance

- **22** days avg. from submission to first decision

Connective Tissue Research

- **Q1** CiteScore Best
- **14** days avg. from

Editorial board

Editor in Chief

Gary Ballian, Ph.D.

Professor Emeritus, University of Virginia

Orthopaedic Research and Biochemistry & Molecular Genetics

Box 800374,

Charlottesville, VA 22908

Phone: (434) 924-2615 or 5181, Fax: (434) 924-1691

Editorial Assistant

Elizabeth Lux

Feinberg Cardiovascular Research Institute

Northwestern University

Chicago, IL

Associate Editors

Andrea I. Alford - *Department of Orthopaedic Surgery, University of Michigan*, Ann Arbor, MI, USA

Salomon Amar - *School of Dental Medicine, Boston University*, Boston, MA, USA

Elizabeth W. Bradley - *Department of Orthopaedic Surgery, University of Minnesota*, Minneapolis, MN, USA

Charles C. Clark - *Department of Orthopaedic Surgery, University of Pennsylvania*, Philadelphia, PA, USA

Chitra L. Dahia - *Hospital for Special Surgery, Weill Cornell Medical College,* New York, NY, USA

Brian O. Diekman - *Department of Biomedical Engineering (University of North Carolina / NC State Univ), Thurston Arthritis Research Center,* UNC, Chapel Hill, NC, USA

Connective Tissue Research

Anne George - *Department of Oral Biology, University of Illinois,* Chicago, IL

About this journal

Buy a subscription

Aims and scope

Journal metrics

Editorial board

Abstracting and indexing

Open access

News and calls for papers

Publication details

Advertising information

Kurt D. Hankenson - *Department of Orthopaedic Surgery, University of Michigan Medical School,*

of Medicine, Kanazawa, Japan

Christine B. Kern - *Department of Regenerative Medicine and Cell Biology, Medical University of South Carolina,* Charleston, SC, USA

Kenneth M. Kozloff - *Department of Orthopaedic Surgery, University of Michigan*, Ann Arbor, MI, USA

Anne-Marie Lang - *Department of Orthopaedic Surgery*, University of Michigan, Ann Arbor, MI, USA

Dianne Little - *Purdue University*, West Lafayette, IN, USA

Amy McNulty - *Department of Orthopaedic Surgery, Duke University School of Medicine*, Durham, NC, USA

Janet Moradian-Oldak - *Center for Craniofacial Molecular Biology, University of Southern California*, Los Angeles, CA, USA

Monzur Murshed - *Department of Medicine and Faculty of Dentistry, McGill University,* Montreal, QC, Canada

Sidney Omelon - *Department of Materials Engineering, McGill University,* Montréal, Québec, Canada

Alberto Passi - *DSCM, Insubria Medical School*, Varese, Italy

M. Farooq Rai - *Biological Sciences, Khalifa University*, Abu Dhabi, United Arab Emirates

Makarand V. Risbud - *Department of Orthopaedic Surgery and Graduate Program in Cell and Developmental Biology, Thomas Jefferson University*, Philadelphia, PA, USA

Lachlan J. Smith - *Departments of Neurosurgery and Orthopaedic Surgery, University of Pennsylvania,* Philadelphia, PA, USA

Dmitriy Sheyn - *Board of Governors Regenerative Medicine Institute, Department of Orthopedics, Cedars-Sinai Medical Center,* Los Angeles, CA, USA

Spencer Szczesny - *Department of Biomedical Engineering, Department of Orthopaedics and Rehabilitation, Pennsylvania State University*, University Park, PA, USA

Simon Tew - *Institute of Life Course and Medical Sciences, University of Liverpool,* UK

Connective Tissue Research

Jay Trivedi - *Department of Orthopaedics, Warren Alpert Medical School of Brown*

About this journal

Buy a subscription

Aims and scope

Madison, WI, USA

Journal metrics

Editorial board

Rochester, NY, USA

Abstracting and indexing

Coiieen Wu - *Departments of Orthopaedics, Ceii Bioiogy, and Pharmacoiogy and Cancer Bioiogy, Duke University*, Durham USA

Open access

News and calls for papers

Updated 12-06-2025

Publication details

Read more about editorial board roles.

Advertising information

Abstracting and indexing

Connective Tissue Research is abstracted/indexed in:

- Academic Search Complete
- BIOBASE
- Biological Abstracts
- Biochemistry and Citation Index
- Biomedical Reference Collection: Comprehensive, Chemical Abstracts, Current Contents -- Life Sciences
- Calcium and Calcified Tissues Abstracts
- Chemical Hazards in Industry
- Chemical Safety Newsbase
- EMBASE
- Embiology
- ETOH
- IBZ

Connective Tissue Research

Open access

Publishing open access means that your article will be free to access online immediately on publication, increasing the visibility, readership, and impact of your research.

Increase the discoverability and readership of your article

Make an impact and reach new readers, not just those with easy access to a research library

Freely share your work with anyone, anywhere

Comply with funding mandates and meet the requirements of your institution, employer or funder

Rigorous peer review for every open access article

Article Publishing Charges

If you choose to publish open access in this journal you may be asked to pay an Article Publishing Charge (APC). You may be able to publish your article at no cost to yourself or with a reduced APC if your institution or research funder has an open access agreement or membership with Taylor & Francis.

If you choose not to publish open access in this journal, there is no APC.

Use our APC finder to calculate your article publishing charge

News, offers and calls for papers

Calls for papers

- 2025 Connective Tissue Research Award

Connective Tissue Research

Would you like to advertise in Connective Tissue Research?

reviewed research by advertising in Connective Tissue Research.

Explore advertising solutions

Taylor & Francis make every effort to ensure the accuracy of all the information (the "Content") contained in our publications. However, Taylor & Francis, our agents (including the editor, any member of the editorial team or editorial board, and any guest editors), and our licensors, make no representations or warranties whatsoever as to the accuracy, completeness, or suitability for any purpose of the Content. Any opinions and views expressed in this publication are the opinions and views of the authors, and are not the views of or endorsed by Taylor & Francis. The accuracy of the Content should not be relied upon and should be independently verified with primary sources of information. Taylor & Francis shall not be liable for any losses, actions, claims, proceedings, demands, costs, expenses, damages, and other liabilities whatsoever or howsoever caused arising directly or indirectly in connection with, in relation to, or arising out of the use of the Content. Terms & Conditions of access and use can be found at http://www.tandfonline.com/page/terms-and-conditions .

Sample our Bioscience Journals

>> Sign in here to start your access to the latest two volumes for 14 days

Connective Tissue Research

Keep up to date

Register to receive personalised research and resources by email

Sign me up

Copyright © 2025 Informa UK Limited Privacy policy Cookies Terms & conditions Accessibility

Taylor and Francis Group

Registered in England & Wales No. 01072954
5 Howick Place | London | SW1P 1WG



Connective Tissue Research

ISSN: 0300-8207 (Print) 1607-8438 (Online) Journal homepage: www.tandfonline.com/journals/icts20

Protective effects of Apelin-13 on steroid-induced osteonecrosis of the femoral head in rats

Ozancan Biçer, Ozan Beytemur, Mustafa Fatih Daşci, Muhammed Uslu, Yiğit Güleryüz, Yiğit Önaloğlu, Emin Can Balci & Büşra Yaprak Bayrak

To cite this article: Ozancan Biçer, Ozan Beytemur, Mustafa Fatih Daşci, Muhammed Uslu, Yiğit Güleryüz, Yiğit Önaloğlu, Emin Can Balci & Büşra Yaprak Bayrak (05 Nov 2025): Protective effects of Apelin-13 on steroid-induced osteonecrosis of the femoral head in rats, Connective Tissue Research, DOI: 10.1080/03008207.2025.2573679

To link to this article: https://doi.org/10.1080/03008207.2025.2573679

Published online: 05 Nov 2025.

Submit your article to this journal

Article views: 64

View related articles

View Crossmark data

Full Terms & Conditions of access and use can be found at
https://www.tandfonline.com/action/journalInformation?journalCode=icts20

CONNECTIVE TISSUE RESEARCH
https://doi.org/10.1080/03008207.2025.2573679

Taylor & Francis
Taylor & Francis Group

Check for updates

Protective effects of Apelin-13 on steroid-induced osteonecrosis of the femoral head in rats

Ozancan Biçer [a], Ozan Beytemur [b], Mustafa Fatih Daşci [a], Muhammed Uslu [a], Yiğit Güleryüz [c], Yiğit Önaloğlu [d], Emin Can Balci [a], and Büşra Yaprak Bayrak [e]

[a]Department of Orthopaedics and Traumatology, Bağcılar Training and Research Hospital, University of Health Sciences, Istanbul, Turkey; [b]Department of Orthopaedics and Traumatology, Medipol Bahçelievler Hospital, Istanbul, Turkey; [c]Department of Orthopaedics and Traumatology, Tatvan State Hospital, Bitlis, Turkey; [d]Department of Orthopaedics and Traumatology, Başakşehir Çam and Sakura City Hospital, Istanbul, Turkey; [e]Department of Pathology, Faculty of Medicine, Kocaeli University, Kocaeli, Turkey

ABSTRACT

Background: Osteonecrosis of the femoral head (ONFH) is a debilitating condition characterized by bone tissue necrosis due to vascular insufficiency, often triggered by corticosteroid use. Steroids are commonly employed in the management of autoimmune diseases, organ transplantation, and COVID-19. Early detection is crucial, as ONFH primarily affects young and middle-aged individuals and often progresses to femoral head collapse if untreated.

Objective: To evaluate the protective effects of Apelin-13 (Ap-13) on steroid-induced ONFH (SONFH) in a rat model.

Methods: Thirty-two female Sprague-Dawley rats were randomized into four groups: Control, Ap-13 only, ONFH, and ONFH + Ap-13. SONFH was induced using lipopolysaccharide (LPS) and methylprednisolone (MPS). The treatment group received daily intraperitoneal Ap-13 injections. At the fourth week, radiological, histopathological, immunohistochemical, and biochemical analyses were conducted on femoral heads.

Results: Micro-CT showed no significant differences in bone mineral density or trabecular parameters. Histopathology revealed increased osteonecrosis, empty lacunae, and vascular thrombosis in the ONFH group, which were significantly reduced in the ONFH + Ap-13 group ($p < 0.05$). Ap-13 decreased serum malondialdehyde (MDA) levels ($p = 0.0002$), reduced caspase-3 expression ($p < 0.05$), and elevated VEGF expression ($p = 0.046$), indicating reduced oxidative stress, apoptosis, and enhanced vascularization. Additionally, LDL and triglyceride levels were significantly lower in the Ap-13 treated group ($p < 0.05$).

Conclusion: Apelin-13 demonstrates protective effects against SONFH by reducing oxidative stress, apoptosis, and improving vascularization. It may represent a promising noninvasive therapeutic strategy for early-stage ONFH.

ARTICLE HISTORY
Received 9 August 2025
Accepted 7 October 2025
Published online 6 November 2025

KEYWORDS
Apelin-13; osteonecrosis; steroid-induced osteonecrosis; femoral head; oxidative stress; apoptosis; vascularization

Introduction

Osteonecrosis (ON), alternatively termed avascular necrosis or aseptic necrosis, is defined as the death of bone cells resulting from compromised blood supply to the bone, originating from either traumatic or non-traumatic causes[1]. ON refers to the death of bone tissue, often linked to circulatory disruption caused by various factors. Notably, corticosteroid use and excessive alcohol consumption account for over 80% of cases. These factors impair femoral blood flow through mechanisms such as vascular endothelial damage and microvascular thrombosis. Additionally, they promote intramedullary adipogenesis, which raises intraosseous pressure, resulting in venous stasis and arterial obstruction. Corticosteroids further contribute to osteonecrosis by reducing osteoblast production, increasing osteocyte apoptosis, and extending the lifespan of osteoclasts[2].

Steroids are widely utilized in the management of chronic autoimmune conditions, including systemic lupus erythematosus, nephrotic syndrome, and asthma, as well as following organ transplantation, in neurological disorders, and in patients hospitalized with novel coronavirus disease 2019 (COVID-19)[3]. The annual incidence of ON in the United States is estimated to range from approximately 20,000 to 30,000 cases, predominantly affecting young adults aged 20 to 40 years[4]. Osteonecrosis of the femoral head accounts for up to % 18 of total hip arthroplasties and the outcomes of total hip arthroplasty in patients with osteonecrosis remain controversial as this patient population is generally

CONTACT Ozancan Biçer bicerozancan@gmail.com Department of Orthopaedics and Traumatology, Bağcılar Training and Research Hospital, University of Health Sciences, Fikirtepe Avenue, Volkan Street, Kadıköy/Istanbul, Turkey

© 2025 Informa UK Limited, trading as Taylor & Francis Group

younger and more active and is therefore associated with higher rates of complications and revision surgeries[5].

Numerous studies have investigated the pathogenic mechanisms underlying steroid-induced osteonecrosis of the femoral head (SONFH). To date, several molecular pathways have been implicated, including apoptosis, oxidative stress, impaired osteogenesis, vasoconstriction, lipid metabolism disorders, and dysregulation of the coagulation and fibrinolysis systems[6].

Apelin/APJ is broadly expressed in various tissues and is involved in the regulation of key physiological and pathological processes, including autophagy, apoptosis, inflammation, and oxidative stress[7]. As a member of the adipokine family, Ap-13 exhibits diverse biological functions and has been implicated in the pathogenesis and treatment of bone diseases. In osteoporosis and fracture healing, Ap-13 exerts osteoprotective effects by modulating autophagy and apoptosis in bone marrow mesenchymal stem cells (BMSC) while promoting their osteogenic differentiation. Moreover, Ap-13 mitigates arthritis progression by regulating macrophage-mediated inflammatory responses. These findings highlight the critical role of Ap-13 in bone protection, offering a novel therapeutic strategy for managing bone-related disorders[8].

This study aimed to investigate the protective role of Ap-13 in preventing SONFH in a rat model. The central hypothesis was that Ap-13 could mitigate the development of SONFH.

Materials and methods

Animals

The study was conducted using 32 young adult female Sprague-Dawley rats, aged 12 weeks, with an average weight of 290 g (range: 275–315 g). The animals were housed under controlled conditions at 22 °C with a 12-hour light/dark cycle. They were provided with unrestricted access to standardized rodent feed and tap water (ad libitum) throughout the study, both before and after drug administration. To ensure the exclusion of any underlying diseases, all rats were observed and monitored for seven days in the animal care laboratory prior to the commencement of the experiment.

Experimental design

SONFH model was established in rats using methylprednisolone (MPS) and lipopolysaccharide (LPS), following established protocols from the literature[9]. Thirty-two rats were randomly divided into four groups, each consisting of eight animals: (I) Control group, (II) Ap-13 group, (III) ONFH group, and (IV) ONFH+ Ap-13 group. To induce ONFH, 16 rats from the ONFH and ONFH+ Ap-13 groups received two intraperitoneal injections of 20 μg/kg LPS (Escherichia coli O55:B5, Sigma-Aldrich, St. Louis, MO, USA) on Days 1 and 2, with a 24-hour interval between doses. Additionally, the same rats were administered three intramuscular injections of 40 mg/kg MPS sodium succinate (Mustafa Nevzat Pharmaceuticals and Chemicals Industry, Istanbul, Turkey) at 24-hour intervals.

The control group received daily intraperitoneal injections of saline solution, beginning on the first day of the protocol. The Ap-13 group was administered 30 μg/kg/day of Ap-13 (Cayman Chemical, Ann Arbor, Michigan, USA) via intraperitoneal injection once daily from the first day. Similarly, the ONFH group received daily intraperitoneal injections of saline starting on the first day to establish the ONFH model. In the ONFH+ Ap-13 group, all rats were administered 30 μg/kg/day of Ap-13 intraperitoneally once a day from the first day of the experiment.

At the end of the fourth week, intracardiac blood samples were collected from all rats for biochemical analysis. Subsequently, the animals were sacrificed under general anesthesia, and their right femurs were surgically extracted. The extracted bones were fixed in 10% formaldehyde for further histological, immunohistochemical, and radiological evaluations.

Radiological examination

All excised femurs were subjected to three-dimensional (3D) scanning and analysis using micro-computed tomography (CT) (SkyScan 1174v2, Kontich, Belgium). Prior to analysis, calibration for bone mineral density (BMD) was performed using a dataset standardized with calcium hydroxyapatite (CaHA) calibration phantoms of 0.25 g/mm^3 and 0.75 g/mm^3. Volumetric ratios were computed separately based on regions of interest (ROIs) and threshold data. Sample data were processed in the CTVol software (v. 2.3.2.0) to generate 3D models.

Using the ROI defined in the femoral head, several parameters were quantified with CTAn software (v. 1.16.4.1+), including BMD (g/cm^3), bone volume/total volume (BV/TV), trabecular thickness (Tb.Th), trabecular number (Tb.N), porosity, trabecular spacing (Tr.Sp.), trabecular separation (Tr. Sep.), trabecular bone pattern factor (Tb.Pf.), and bone surface area/bone volume ratio (BS/BV). The following microarchitectural trabecular parameters were evaluated as follows:

- Trabecular Number (Tb.N, mm^{-1}): Represents the number of trabeculae per unit length; it reflects how many trabeculae are present within a given region and is indicative of trabecular density.
- Trabecular Spacing (Tb.Sp, mm): Indicates the mean distance between trabeculae; increased values suggest a loss of trabecular bone.
- Trabecular Separation (Tb.Sep, mm): Similar to trabecular spacing, this metric reflects the average distance between individual trabeculae and is often used interchangeably with Tb.Sp.
- Trabecular Bone Pattern Factor (Tb.Pf, mm^{-1}): A measure of trabecular connectivity; higher values indicate more disconnected or isolated trabeculae, which is characteristic of deteriorating bone microarchitecture.

Histopathological examination

The tissue sections were initially fixed in 10% buffered formaldehyde solution and subsequently decalcified in a 10% formic acid solution for three days. Following routine tissue processing, the samples were embedded in paraffin blocks. Longitudinal sections of 3–4 µm thickness were prepared and stained using hematoxylin-eosin (H&E) and Masson's trichrome methods. Histopathological examination was conducted under a light microscope (Zeiss Axio microscope with Zen 2.3 Lite software), and images were captured with an attached camera (AxioCam IC). The pattern of bony trabeculae was evaluated based on architectural integrity as follows:

- Regular trabeculae were continuous and thick, with uniform arrangement and preserved alignment.
- Partially irregular trabeculae exhibited mild focal discontinuity or uneven alignment but retained general structure.
- Irregular trabeculae showed disorganized orientation, fragmented structure, or architectural distortion.
- Thin trabeculae were defined as having visibly reduced width compared to surrounding trabeculae, often with atrophic appearance.

Osteocyte density was assessed by counting nuclei per high-power field (HPF):

- Marked osteocytes indicated a dense population of osteocyte nuclei within trabeculae, generally ≥10 nuclei per HPF.
- Sparse osteocytes referred to significantly fewer nuclei, typically < 5 per HPF, indicating osteocyte depletion.

Adipocyte morphology in bone marrow was evaluated semi-quantitatively:

- Large adipocytes were defined as adipocytes with ≥1.5× diameter compared to average marrow adipocytes in the control group.
- Increased adipocytes referred to increased adipocyte number per field compared to control, usually a > 30% increase in adipocyte density.

The presence of macrophages in the bone marrow was recorded as increased if clusters or sheets of macrophages were observed in ≥ 2 HPFs, verified by morphological criteria including eccentric nuclei and vacuolated cytoplasm.

Immunohistochemical examination

To investigate cellular oxidative damage in femoral head tissue, transforming growth factor-ß (TGF-ß) was used as a marker. Malondialdehyde (MDA) was employed to assess lipid peroxidation levels. Anti-apoptotic protein Bcl-2 and pro-apoptotic protein caspase-3 were analyzed to evaluate apoptotic pathways, and vascular endothelial growth factor (VEGF) was used to detect vascular damage. Additionally, bone morphogenetic proteins-4 (BMP-4) and bone morphogenetic proteins-7 (BMP-7), along with their corresponding antibodies, were utilized to demonstrate bone healing following ON. Immunohistochemical staining was performed using the Streptavidin-biotin-peroxidase method with these specific monoclonal and polyclonal antibodies[9,10].

Biochemical examination

Intracardiac blood samples were collected immediately after sacrification for hematological analysis. The samples were centrifuged at 3,000 rpm for 10 minutes, and the serum was stored at −80 °C until further analysis. Biochemical parameters, including serum levels of malondialdehyde (MDA), glutathione (GSH), bone alkaline phosphatase (BALP), osteoprotegerin (OPG), triglycerides (TG), total cholesterol (TC), high-density lipoprotein cholesterol (HDL), and low-density lipoprotein cholesterol (LDL), were measured using enzyme-linked immunosorbent assay (ELISA) with double antibody sandwich technology.

Statistical analysis

Statistical analyses were conducted using GraphPad Instat software, version 3.06 (GraphPad Inc., CA, USA). Continuous data were expressed as mean ± standard deviation (SD), while categorical variables were presented as numbers and frequencies. The Kolmogorov-Smirnov test was used to assess the normality of data distribution.

Categorical variables were analyzed using the chi-square test for independence. Normally distributed numerical variables were compared using one-way analysis of variance (ANOVA), followed by Tukey-Kramer multiple comparison test as a post-hoc analysis. For non-normally distributed numerical variables, the Kruskal-Wallis test (non-parametric ANOVA) was used, with Dunn's multiple comparison test applied post-hoc. Statistical significance was defined at p-values of < 0.05, < 0.01, and < 0.001.

Results

Radiological findings

In the ONFH model, radiological measurements, including BMD, BV/TV, Tb.Th, Tb.N, Tb.Pf, and BS/BV ratios, were performed on radiological images obtained after femoral head scans (Figure 1) to assess the radiological effects of Ap-13. Although these parameters showed a decrease in the ONFH group compared to the control group, no statistically significant differences were observed between the groups ($p > 0.05$) (Table 1).

Histopathological findings

The diagnosis of ON was established based on the presence of empty lacunae in bone trabeculae or osteocytes with pyknotic nuclei, accompanied by necrosis

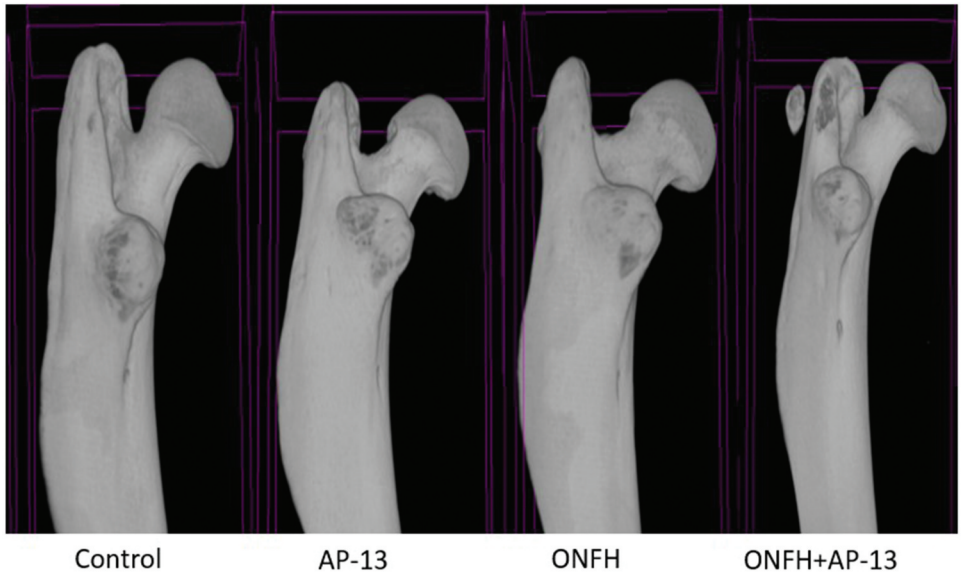


Figure 1. Micro-CT images of the femoral heads of 8 rats in which SONFH model established.

Table 1. The distribution of radiological findings of femoral head sections by group ($n = 8$) and statistical comparison.

	Control	AP-13	ONFH	ONFH+AP-13	P Value
Radiological findings			*X ± SD*		
BMD (g/cm^3)	1.23 ± 0.05	1.22 ± 0.04	1.20 ± 0.02	1.723 ± 0.04	0.536
BV/TV (%)	95.51 ± 1.68	95.35 ± 1.41	94.12 ± 1.80	94.88 ± 1.88	0.525
Tb. Th (mm)	0.68 ± 0.15	0.65 ± 0.11	0.57 ± 0.07	0.62 ± 0.09	0.382
Tb. N (mm^{-1})	49.56 ± 3.23	47.60 ± 6.81	49.26 ± 4.73	49.81 ± 2.80	0.766
Tb. Sp (mm^{-1})	1.46 ± 0.24	1.45 ± 0.21	1.58 ± 0.24	1.52 ± 0.18	0.645
Tb. Sep (mm)	0.12 ± 0.02	0.12 ± 0.01	0.15 ± 0.05	0.16 ± 0.08	0.495
Tb.Pf. (mm^{-1})	−9.88 ± 1.83	−10.77 ± 1.92	−11.13 ± 2.18	−11.44 ± 1.81	0.417
BS/BV (mm^{-1})	4.32 ± 0.84	4.05 ± 0.48	3.54 ± 0.41	3.88 ± 0.46	0.099

X ± SD: Mean ± Standard deviation. BMD (g/cm^3), bone volume/total volume (BV/TV), trabecular thickness (Tb.Th), trabecular number (Tb.N), porosity, trabecular spacing (Tr.Sp.), trabecular separation (Tr.Sep.), trabecular bone pattern factor (Tb.Pf.), and bone surface area/bone volume ratio (BS/BV).

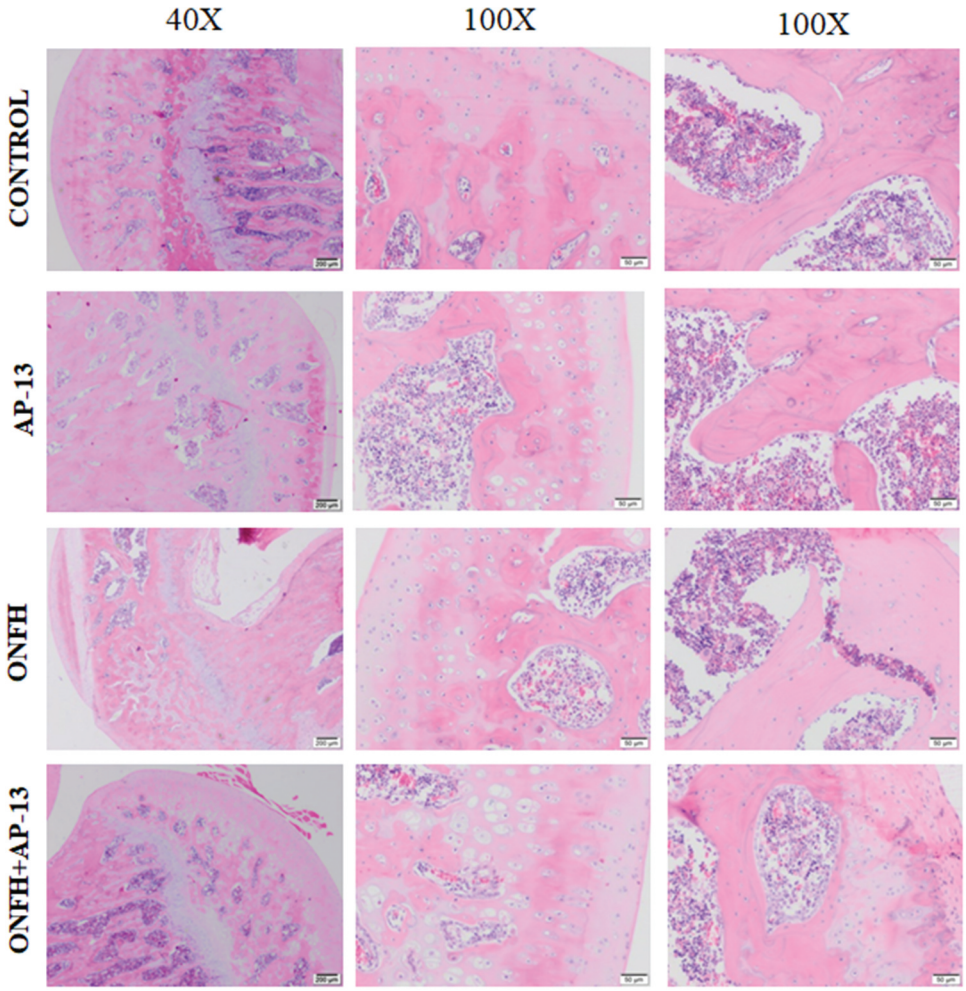


Figure 2. Light microscopic images of femoral head sections in the SONFH model established in 8 rats. Two representative 100× images from different regions of the femoral head are shown to illustrate trabecular and marrow changes. Hematoxylin + eosin, 40x and 100x magnification.

with a diffuse distribution, as observed under light microscopy (Figure 2).

In the ONFH group, prominent necrotic areas, anomalies, and pale regions were identified in the femoral head compared to the control and AP-13 groups. Additionally, in many samples, bone trabeculae were observed to be locally thinned, irregular, and intermittently arranged, with voids forming in the tissue compared to the control group. Sparse osteocytes, numerous pyknotic cells, and empty lacunae were detected in the trabeculae. Furthermore, the bone marrow in the ONFH group showed a loss of normal morphology compared to the control group, with a reduction in bone marrow cells in most samples. Thrombus, hematopoietic cell necrosis, and hemorrhage were also observed in the bone marrow of all animals in the ONFH group (Table 2).

In the ONFH+AP-13 group, a reduction in ON and anomalies in the femoral head was observed compared to the ONFH group. In half of the animals, bone trabeculae maintained an intact and regular structure similar to the control group, with voids and gaps no longer present. The number of osteocytes in the trabeculae returned to normal, while the number of pyknotic cells and empty lacunae decreased. In the ONFH+AP-13 group, while osteonecrotic features were markedly reduced, granulation tissue and fibrosis were observed in 4 out of 8 animals, which was comparable in incidence to the ONFH group. This suggests that despite the attenuation of necrotic damage, tissue remodeling and reparative responses were still ongoing in the Ap-13 treated group (Table 2).

The proportion of animals with ON and femoral head anomalies was found to be significantly higher in the ONFH group compared to other groups, while it significantly decreased in the ONFH+AP-13 group ($p = 0.0137$ for both comparisons). When the histopathological parameters of bone trabeculae were compared, the number of subjects with irregular, thin, and intermittently spaced trabeculae with voids was

Table 2. Comparison of histopathological findings of femoral head sections according to groups ($n = 8$) of SONFH model.

	Control	AP-13	ONFH	ONFH+AP-13	P Value
Parameters			*X/N*		
Osteonecrosis	0/8	0/8	8/8	4/8	**0.0137**
Femur head anomaly	0/8	0/8	8/8	4/8	**0.0137**
Bone trabeculae	8/8	5/8	0/8	3/8	**0.0007**
Regular	0/8	2/8	3/8	4/8	0.1441
Partially regular	0/8	1/8	5/8	1/8	**0.0129**
Irregular	0/8	3/8	7/8	5/8	**0.0038**
Thin	0/8	1/8	5/8	1/8	**0.0129**
Intermittent/space	0/8	1/8	4/8	1/8	0.0606
Fractured	0/8	4/8	8/8	4/8	**0.0011**
Granulation	0/8	5/8	7/8	5/8	**0.0038**
Fibrosis					
Osteocytes	8/8	7/8	3/8	5/8	**0.0277**
Marked	0/8	1/8	5/8	3/8	**0.0277**
Sparse					
Bone marrow	7/8	5/8	0/8	1/8	**0.0007**
Normal	2/8	2/8	3/8	5/8	0.3618-**0.0016**
Increased adipocyte	0/8	0/8	0/8	0/8	**0.0155**
Large adipocytes	2/8	5/8	8/8	8/8	**0.0066**
Hemorrhage	2/8	5/8	8/8	6/8	0.2909
Thrombus	3/8	8/8	8/8	6/8	0.3618
Macrophage	2/8	2/8	3/8	2/8	**0.0426**
Increased HC	2/8	2/8	5/8	3/8	
Decreased HC	0/8	2/8	5/8	4/8	
HC necrosis					
			X ± SD		
Pyknotic cell (%)	1.62 ± 1.06	17.62 ± 15.31[a]	31.00 ± 13.02[b]	17.88 ± 10.57[a]	**0.0002**
Empty lacunae (%)	7.38 ± 3.78	20.83 ± 11.02	26.14 ± 9.35[c]	18.75 ± 13.29	**0.0090**
Vascular thrombosis (%)	2.25 ± 4.20	17.5 ± 12.24	56.63 ± 16.03[b.d]	22.50 ± 16.47	**0.0001**

X/n: Number of animal with pathology/total number of animals; HC: Hematopoietic cells; SD: Standard deviation; X ± SD: Mean ± Standard deviation. *p < 0.05 vs. control group. [a]P < 0.05, [b]P < 0.001, [c]P < 0.01 vs. control group [d]P < 0.05 vs. AP-13 group.

significantly higher in the ONFH group compared to the control group, whereas it was lower in the ONFH +AP-13 group ($p < 0.05$). Additionally, the number of subjects with regular trabeculae was significantly higher in the control and AP-13 groups compared to other groups ($p = 0.0007$) (Table 2).

In the ONFH group, granulation tissue was observed in all subjects, and fibrosis was detected in seven subjects. However, in the treatment group, both granulation tissue and fibrosis were found to be significantly reduced ($p < 0.05$). When the histopathological parameters of bone marrow were compared, no animals in the ONFH group exhibited normal morphology. Hemorrhage, thrombus, and hematopoietic cell necrosis, accompanied by numerous macrophages, were significantly increased in all animals of the ONFH group compared to other groups ($p < 0.05$) (Table 2).

No statistically significant differences were observed among the groups in terms of the quantity and size of adipocytes ($p > 0.05$). The proportions of pyknotic cells, empty lacunae, and vessels with thrombus in the trabeculae were significantly higher in the ONFH group compared to the control group ($p < 0.05$). However, these proportions decreased in the ONFH +AP-13 group, with the rates of empty lacunae and vascular thrombus resembling those of the control group (Table 2).

Immunohistochemical findings

In the ONFH group, BMP-4 levels in adipocytes and trabeculae were significantly increased compared to the control group ($p = 0.0327$ and $p = 0.0063$, respectively), whereas the increase in bone marrow was not statistically significant ($p = 0.1436$). In the ONFH+AP-13 group, BMP-4 levels in adipocytes and trabeculae returned to normal levels (Figures 3 and 4).

No significant differences were observed between the control group and the AP-13 or ONFH+AP-13 groups ($p > 0.05$). When BMP-7 immunoreactivity was examined, BMP-7 levels in adipocytes, bone marrow, and trabeculae of the ONFH group were found to be significantly lower compared to the control group. However, in the ONFH +AP-13 group, BMP-7 levels were significantly increased compared to the AP-13 group ($p = 0.0009$, $p = 0.004$, and $p = 0.036$, respectively). No differences in BMP7 immunoreactivity were observed between the control group and the AP-13 group ($p > 0.05$) (Figures 3 and 4).

To evaluate apoptotic pathways, the immunoreactivity of the anti-apoptotic protein Bcl-2 was examined. In the ONFH group, most subjects showed no Bcl-2 immunoreactivity in adipocytes, bone marrow, or trabeculae, whereas a slight increase was observed in the ONFH+AP-13 group. However, no statistically

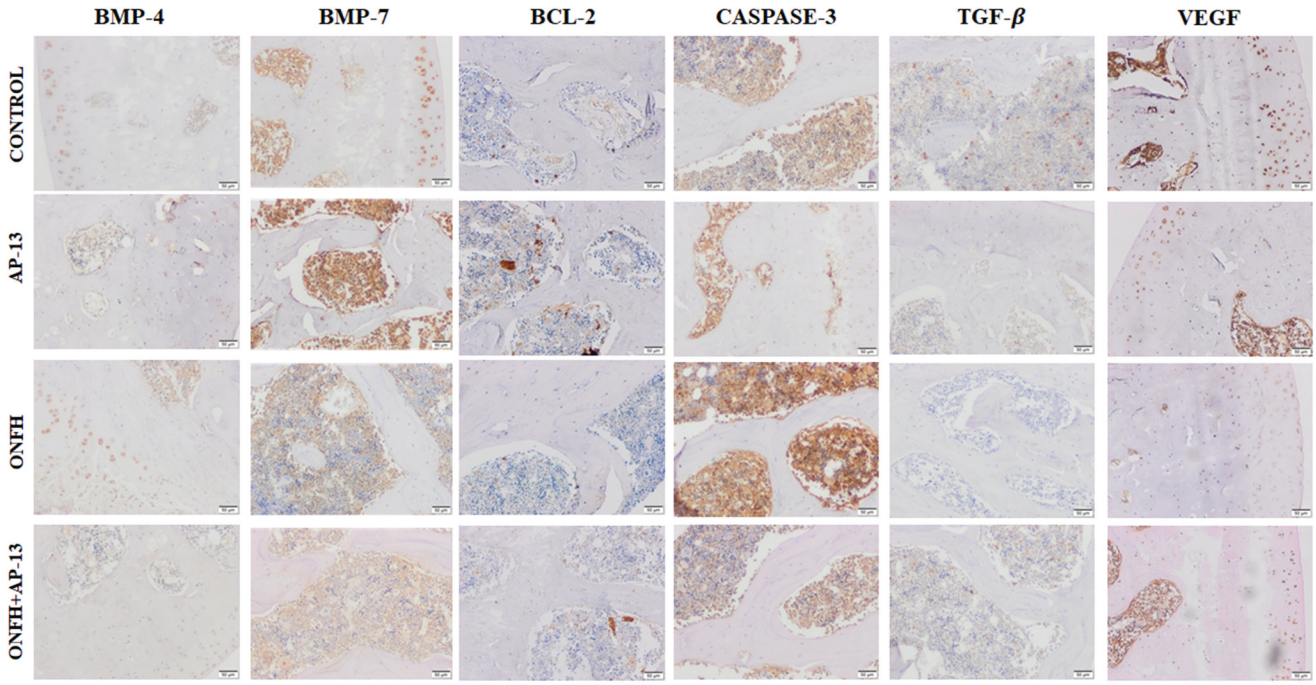


Figure 3. Light microscopic images of immunohistochemistry analysis of femoral head sections in osteonecrosis of femoral heads of 8 rats.100x magnification.

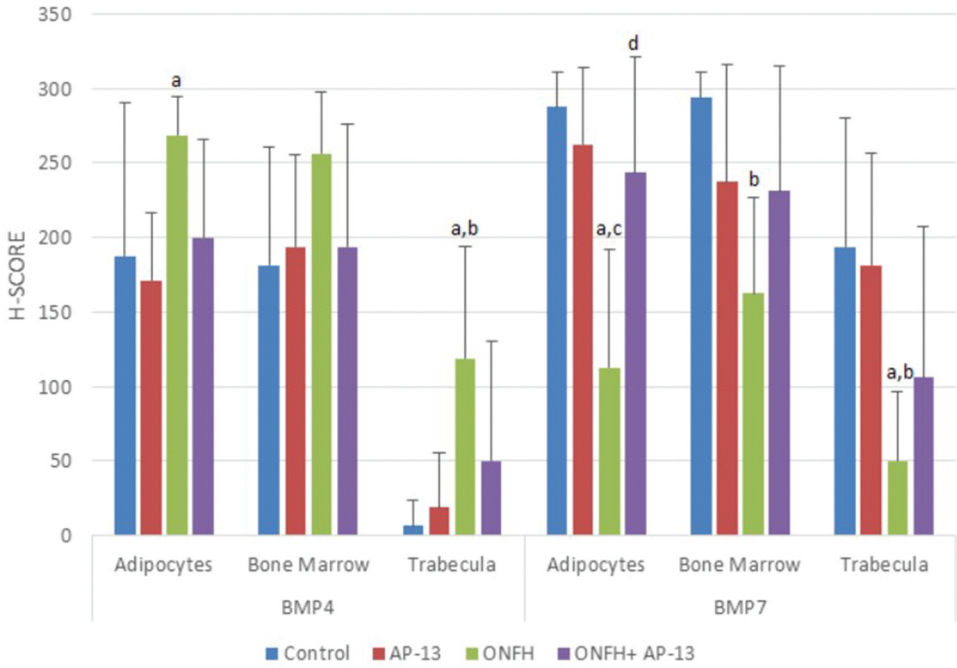


Figure 4. BMP-4 and BMP-7 immunoreactivities in femoral head sections and statistical comparison by group ($n = 8$). $p = 0.0327$ for BMP-4 in adipocytes; $p = 0.1436$ for BMP-4 in bone marrow; $p = 0.0063$ for BMP-4 in trabeculae. $p = 0.0009$ for BMP-7 in adipocytes; $p = 0.004$ for BMP-7 in bone marrow; $p = 0.036$ for BMP-7 in trabeculae. A $p < 0.05$ vs corresponding AP-13 group; b $p < 0.01$ and c $p < 0.001$ vs corresponding control group; d $p < 0.05$ vs corresponding ONFH group.

significant differences were found between the groups ($p > 0.05$) (Figures 3 and 5).

When the immunoreactivity of the pro-apoptotic protein caspase-3 was examined, its levels in the bone marrow and trabeculae were found to be significantly increased in the ONFH group compared to the control group ($p < 0.05$). In the ONFH+AP-13 group, these levels returned to control levels. Similarly, caspase-3

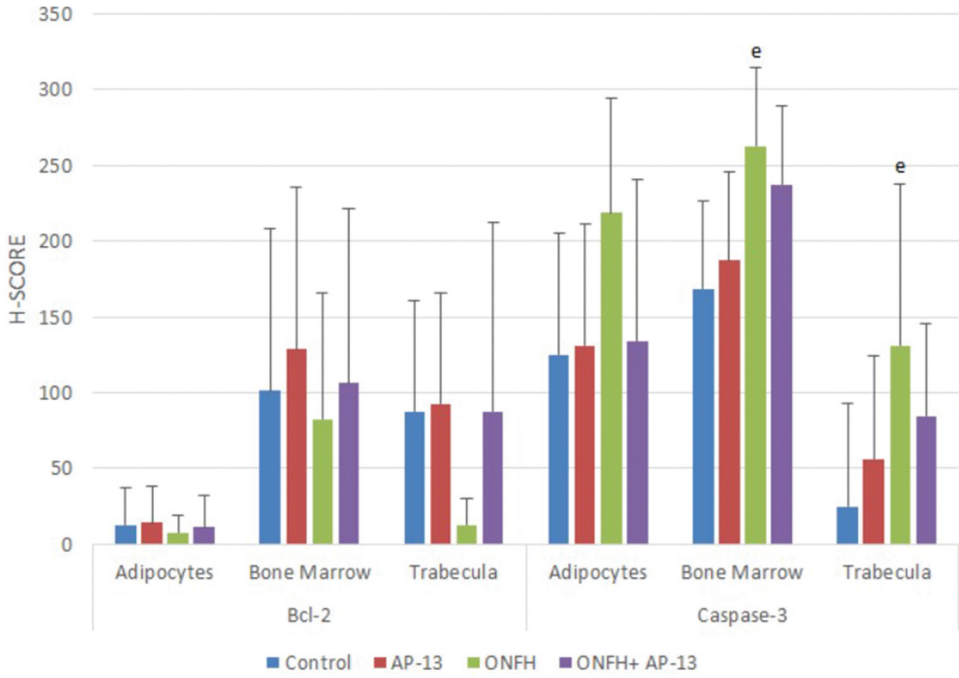


Figure 5. Bcl-2 and caspase-3 immunoreactivities in femoral head sections and statistical comparison by group ($n = 8$). $p = 0.9283$ for Bcl-2 in adipocytes; $p = 0.8138$ for Bcl-2 in bone marrow; $p = 0.2669$ for Bcl-2 in trabeculae. $p = 0.1348$ for caspase-3 in adipocytes; $p = 0.0192$ for caspase-3 in bone marrow; $p = 0.0485$ for BMP-7 in trabeculae. e $p < 0.05$ vs corresponding control group.

levels in the AP-13 group were comparable to those of the control group ($p < 0.05$) (Figures 3 and 5).

In the ONFH group, the mean TGF-β level was lower compared to the other groups; however, no statistically significant differences were observed between the groups ($p > 0.05$). In the treatment group, the mean TGF-β levels were higher than those in the other groups, but this increase was also not statistically significant ($p > 0.05$) (Figures 3 and 6).

In the ONFH group, the mean VEGF levels in endothelial cells were found to be significantly decreased, whereas in the ONFH+AP-13 group, the mean VEGF levels were significantly increased ($p = 0.046$). In the AP-13 group, the mean VEGF levels were similar to those of the control group (Figures 3 and 6).

Biochemical findings

To evaluate systemic oxidative stress and the corresponding antioxidant mechanisms, serum MDA and GSH levels were analyzed using the ELISA method. In the ONFH group, serum MDA levels were significantly increased compared to other groups ($p < 0.05$) and were found to decrease in the ONFH+AP-13 group ($p = 0.0002$). Serum GSH levels in the ONFH group were lower than in other groups, but this decrease was not statistically significant ($p > 0.05$). Serum BALP levels showed no significant differences between the groups ($p = 0.3384$). However, OPG levels were significantly higher in the AVN group compared to the control group and decreased in the ONFH+AP-13 group ($p = 0.0167$). (Table 3)

To evaluate the effects of AP-13 on lipid profiles, serum levels of TC, HDL cholesterol, LDL cholesterol, and triglycerides (TG) were measured using the ELISA method. In the ONFH group, serum TC levels were slightly elevated compared to other groups; however, no significant differences were observed between the groups. Similarly, serum HDL levels showed no significant differences among the groups ($p > 0.05$). Serum LDL and TG levels in the ONFH group were significantly higher compared to the control group, but the levels in the ONFH+AP-13 group approached those of the control group ($p = 0.0143$ and $p = 0.0394$, respectively). Additionally, serum LDL and TG levels in the AP-13 group were found to be similar to those of the control group (Table 4).

Discussion

In this study, we demonstrated that Ap-13 exerts a multifaceted protective effect in a SONFH model. Specifically, Ap-13 significantly reduced oxidative stress, as evidenced by lower MDA levels, and exerted

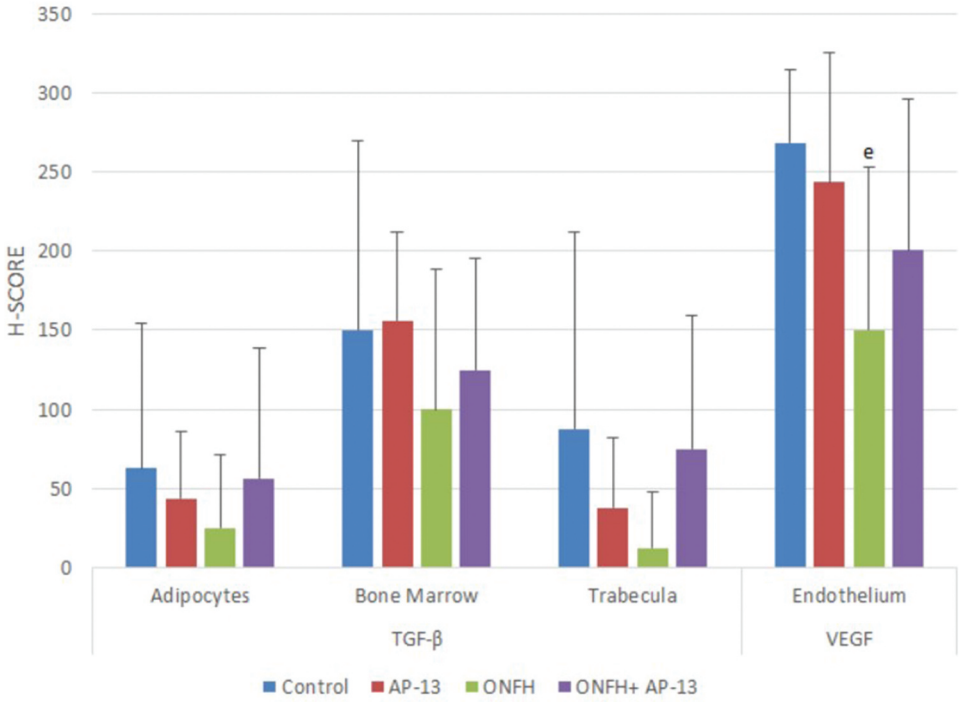


Figure 6. TGF-β immunoreactivities in femoral head sections and VEGF immunoreactivities in endothelium and statistical comparison by group ($n = 8$). $p = 0.7679$ for TGF-β in adipocytes; $p = 0.5614$ for TGF-β in bone marrow; $p = 0.2911$ for TGF-β in trabeculae. $p = 0.0460$ for VEGF in endothelium. e $p < 0.05$ vs corresponding control group. $p = 0.046$.

Table 3. Serum levels of biochemical parameters and comparison by group ($n = 8$).

	Control	AP-13	ONFH	ONFH+AP-13	P Value
Parameter			*X ± SD*		
MDA (nmol/mL)	19.50 ± 2.83	14.12 ± 2.72[a]	13.26 ± 2.78[b]	13.24 ± 2.70[b]	**0.0002**
GSH (mg/L)	272.55 ± 32.08	277.68 ± 72.46	245.40 ± 20.81	246.16 ± 45.15	0.5621
BALP (ng/mL)	1.17 ± 0.38	1.28 ± 0.13	1.41 ± 0.14	1.36 ± 0.30	0.3384
OPG (ng/ml)	1.57 ± 0.47	1.95 ± 0.38	2.18 ± 0.18[c]	2.02 ± 0.23	**0.0167**

X ± SD: Mean ± Standard Deviation, MDA: Malondialdehyde, GSH: Glutathione, BALP: Bone Alkaline Phosphatase, OPG: Osteoprotegerin [a]p < 0.01, [b]p < 0.001, [c]p < 0.05 vs control group.

Table 4. Serum levels of lipid parameters and comparison by group ($n = 8$).

	Control	AP-13	ONFH	ONFH+AP-13	P Value
Parameter			*X ± SD*		
TC (µmol/L)	69.25 ± 8.78	71.5 ± 2.81	73.28 ± 5.02	69.75 ± 8.58	0.6881
HDL (µmol/L)	52.62 ± 7.46	58.37 ± 9.53	54.00 ± 6.97	50.75 ± 6.22	0.2497
LDL (mmol/L)	7.50 ± 1.60	8.25 ± 1.67	9.75 ± 1.28[a]	9.43 ± 0.98	**0.0143**
TG (µmol/L)	71.37 ± 15.46	88.25 ± 26.58	105.28 ± 26.21[a]	77.75 ± 20.66	**0.0394**

X ± SD: Mean ± Standard Deviation, TG: Serum triglyceride, TC: total cholesterol, HDL: High density lipoprotein, LDL: Low density lipoprotein. [a]p < 0.05 vs control group.

anti-apoptotic effects through the suppression of caspase-3 expression. In addition, VEGF immunoreactivity in endothelial cells was markedly increased in the Ap-13 treatment group, suggesting enhanced angiogenesis and vascular repair. Although some parameters—such as pyknotic cell count, empty lacunae percentage, and certain lipid profile markers—showed numerically close mean values between the ONFH and ONFH+Ap-13 groups, statistically significant differences were detected due to consistent intergroup trends and low intra-group variability, as confirmed by post-hoc testing. These findings suggest that Ap-13 elicits meaningful biological effects, even in cases where gross numerical changes appear subtle. Importantly, Ap-13

also normalized OPG levels and improved trabecular architecture, as reflected in histopathological evaluations.

ON, particularly affecting the femoral head, leads to severe bone damage, subchondral bone collapse, and hip joint destruction. It arises from multiple etiological factors, with glucocorticoid therapy identified as a primary predisposing factor. The pathogenesis of SONFH includes ischemia, vascular compromise, and apoptosis[1,2,9]. However, it should be emphasized that the pathogenesis of osteonecrosis of the femoral head is multifactorial, involving vascular impairment, intravascular coagulation, lipid metabolism disorders, and genetic as well as immunological factors, rather than a single mechanism[11]. In our study, we conducted radiological, histopathological, histomorphometric, immunohistochemical, and biochemical analyses to evaluate the efficacy and systemic effects of Ap-13, a peptide secreted by adipose tissue[12], in a SONFH model in rats. The therapeutic effects of Ap-13 were assessed for its antioxidant, anti-osteoclastic, osteoblastic, osteoprotective, and hypolipidemic properties on osteonecrotic areas[7]. Therefore, while our study provides evidence for the vascular and anti-apoptotic protective role of Apelin-13, further investigations are needed to clarify its interactions with other pathogenic pathways.

Interestingly, although Ap-13 administration mitigated many features of osteonecrosis, such as empty lacunae, pyknotic nuclei, and vascular thrombosis, granulation tissue and fibrosis were still observed in several specimens within the Ap-13 group, at rates comparable to the ONFH group. This finding may reflect a transition phase between active injury and reparative response rather than ongoing necrosis. Granulation tissue, which consists of proliferating fibroblasts, neovascularization, and inflammatory cells, often arises as part of a healing process following tissue injury. Similarly, fibrosis may represent reactive scarring and remodeling in response to prior steroid-induced microdamage. The presence of these changes, even in the absence of severe osteonecrotic features, suggests that Ap-13 May reduce acute damage but not entirely suppress the underlying reparative remodeling process, especially within the 4-week experimental timeframe. Longitudinal studies with extended observation periods are warranted to determine whether these fibrotic changes resolve over time or persist.

Oxidative stress is strongly associated with the development of SONFH. Pathological studies in SONFH patients have revealed that prolonged use of glucocorticoids can result in oxidative damage and apoptosis of osteocytes[13]. Tao et al. reported that exosomes derived from platelet-rich plasma (PRP) prevented apoptosis induced by glucocorticoid-associated oxidative stress in rat femoral head necrosis through the Akt/Bad/Bcl-2 signaling pathway[14]. MDA is a product of lipid peroxidation, while GSH serves as one of the most critical antioxidants within the organism. A reduction in GSH levels accompanied by an elevation in MDA levels collectively represents a significant marker of oxidative stress and cellular damage[15]. In our study, an analysis of MDA levels revealed a significant increase in the ONFH model compared to all other groups. Furthermore, it was observed that Ap-13 treatment significantly reduced serum MDA levels, particularly when compared to the untreated ONFH group of rats.

GSH is a vital antioxidant enzyme in vivo, playing a crucial role in maintaining membrane integrity, preserving cellular structure, and facilitating the metabolism of xenobiotics. A reduction in GSH levels leads to the induction of oxidative stress, increasing the susceptibility of the organism to tissue and vascular damage[16]. Geng et al. observed a significant decrease in GSH levels shortly after steroid administration in rats with an osteonecrosis model they developed[17]. In our study, we found that serum GSH levels decreased in the ONFH model but increased with Ap-13 treatment. However, the results were not statistically significant. These findings suggest that the therapeutic effect of Ap-13 on SONFH may be attributed to its ability to inhibit lipid peroxidation and associated oxidative stress, thereby enhancing the antioxidant mechanism.

BALP, a biochemical marker, is used to evaluate bone resorption and formation. It is also employed to predict fracture risk and monitor osteoporosis treatment independently of BMD[18]. When mesenchymal stem cells are stimulated for osteogenesis, they differentiate into osteoblasts, and BALP levels, an important indicator of this differentiation, reflect the presence and maturation of osteoblasts. BALP hydrolyzes organophosphates, increasing local phosphate concentrations and initiating calcification[19].

Zhou et al. demonstrated increased BALP levels in the third week of treatment in rats with SONFH treated with valproic acid[20]. Osteoclastic OPG exerts its effects through the OPG/RANK/RANKL system, with OPG and RANKL produced by osteoblast-derived cells. These glycoproteins, part of the tumor necrosis factor receptor superfamily, are key regulators of bone metabolism[21]. Studies have shown that the ratio of anti-osteoclastogenic cytokine OPG to osteoclastogenic cytokine RANKL is critical for osteoclast activity. Peng et al. observed decreased OPG levels in rats with SONFH[22]. In our study, serum BALP levels did not differ significantly among groups. However, OPG levels

were significantly increased in the AVN group compared to the control group and decreased in the treatment group.

SONFH is suggested to result from osteocyte apoptosis, leading to a cumulative and irreversible disorder. Apoptosis disrupts the unique mechanoreceptor role of the osteocyte-canalicular network, inevitably causing femoral head collapse[23]. Weinstein et al. reported that femoral head sections obtained from patients undergoing total hip arthroplasty due to SONFH contained numerous apoptotic osteocytes, whereas sections from traumatic or sickle cell ON cases showed fewer apoptotic bone cells. This finding suggests that may SONFH primarily involve osteocyte apoptosis[24]. Prolonged and excessive use of steroids alters the microenvironment of osteoblasts and bone mesenchymal stem cells in the femoral head, leading to the overexpression of apoptosis-related factors such as BCL-2, Bax, cytochrome C, caspase-3, and caspase-9. These apoptotic factors trigger a series of reactions that result in cell apoptosis and tissue destruction[25]. In a study by Sun et al., increased caspase-3 levels were observed in rats with SONFH[26]. In our SONFH model, the immunoreactivity of the anti-apoptotic protein Bcl-2 was examined. While most adipocytes, bone marrow, and trabeculae in the ONFH group showed no Bcl-2 immunoreactivity, a slight increase was observed in the treatment group, but the difference between groups was not statistically significant. Regarding the pro-apoptotic protein caspase-3, no statistically significant differences were found among groups in adipocytes. However, caspase-3 levels in the bone marrow and trabeculae of the ONFH group were significantly higher than in the control group. In the ONFH+AP-13 group, these levels returned to control levels, while caspase-3 levels in the AP-13 group were also similar to those of the control group.

Beyond reducing bulk oxidative stress, accumulating evidence indicates that bone-cell reactive oxygen species (ROS) is tightly governed by the ROS/Keap1/Nrf2 axis, which in turn shapes osteoclastogenesis. Multiple natural agents suppress osteoclast differentiation and bone loss by stabilizing or activating Nrf2 and enhancing downstream antioxidant enzymes (e.g., HO-1, NQO1, CAT) while dampening RANKL-driven ROS signaling and NF-κB/MAPKs. For example, tussilagone inhibits mitochondrial ROS production, prevents NFATc1 induction, and up-regulates Nrf2 (genetic loss of Nrf2 blunts its effect) in vitro, and attenuates OVX/LPS-induced bone loss in vivo[27]. Corynoline similarly suppresses RANKL-induced osteoclastogenesis by inhibiting NF-κB/MAPKs and stabilizing Nrf2 to curb ROS, restoring trabecular microarchitecture in OVX mice[28]. Mechanistically convergent strategies—such as direct Keap1–Nrf2 disruption—also restrain osteoclastogenesis and prevent OVX-induced bone loss by activating Nrf2 and limiting ROS-dependent IκB/NF-κB signaling[29]. In addition, 4-methylcatechol has been reported (via docking and cell assays) to act along the RANKL-mediated ROS/Keap1/Nrf2 axis, up-regulating HO-1 and countering osteoclastogenesis, while alpinetin reduces inflammatory bone loss by curbing ROS-dependent p38/PI3K signaling in osteoclasts[30,31]. In this context, our data show that Apelin-13 significantly lowers MDA (with a trend toward higher GSH), reverses caspase-3 increases, enhances endothelial VEGF immunoreactivity, and improves trabecular architecture. These effects plausibly intersect the ROS/Keap1/Nrf2 axis: by lowering ROS, Ap-13 May favor Nrf2 activation (or reduce Keap1-mediated Nrf2 turnover), thereby secondarily restraining RANKL-driven osteoclast programs. Although Ap-13 normalized OPG levels in our model, we did not directly assay the RANKL/OPG balance or Nrf2 pathway readouts (e.g., nuclear Nrf2, HO-1/NQO1). Future work should quantify these endpoints (including Keap1–Nrf2 interaction and RANKL-evoked ROS kinetics) to determine whether Ap-13 acts as an antioxidant modulator of the Keap1/Nrf2 axis in SONFH.

The exact pathophysiology of SONFH remains unclear, but it is generally accepted that reduced blood flow, increased intraosseous pressure, and various metabolic and local factors play significant roles. VEGF is a crucial factor in angiogenesis and bone repair processes. VEGF expression, which regulates angiogenesis supporting the vascular system as well as bone formation and repair, decreases in conjunction with increased osteoblast and osteocyte apoptosis[32]. There are reports of ON occurring in various regions following anti-VEGF treatments, such as bevacizumab[33]. Song et al. observed increased VEGF levels accompanied by enhanced femoral head perfusion while investigating the therapeutic effects of sildenafil in a rabbit ONFH model[34]. Ozmen et al. found an increase in VEGF levels while investigating the effects of tadalafil on ONFH in rabbits but interpreted this as an independent effect of tadalafil rather than an indicator of angiogenesis and osteogenesis[35]. In our study, VEGF levels in endothelial cells were significantly reduced in the ONFH group, whereas they were significantly increased in the ONFH+AP-13 group.

Prolonged administration elevates blood lipid levels, leading to abnormal lipid distribution, fat embolism in microvessels, fat accumulation in the medullary cavity, enlarged fat cell volume, and increased medullary cavity

pressure. Steroids can also disrupt bone microcirculation by causing lipid deposition in bone cells, ultimately resulting in cell death. Hormone-induced lipid metabolism disorders contribute to ONFH through two primary mechanisms: microvascular fat embolization and fatty deposition in osteocytes[36]. An epidemiological study revealed a correlation between elevated LDL levels and the risk of non-traumatic ONFH. Moreover, high LDL is considered an independent risk factor for postoperative ONFH following femoral neck fractures. However, the exact pathophysiology of LDL in ONFH remains unclear[37]. Chen et al. observed that erythropoietin treatment in rats with SONFH resulted in lower TC and triglyceride levels compared to the control group[10]. In our study, while the serum TC levels in the ONFH group were slightly elevated compared to other groups, no significant differences were detected. Similarly, serum HDL levels did not show statistically significant differences among the groups. However, serum LDL and TG levels were significantly higher in the ONFH group compared to the control group, whereas these levels in the ONFH-AP -13 group approached those of the control group. Additionally, serum LDL and TG levels in the AP-13 group were found to be similar to those of the control group.

Bone morphogenetic proteins (BMPs) are members of the TGF-β superfamily, playing crucial roles in various functions such as embryonic development, and cellular processes like growth, differentiation, and apoptosis[38]. BMP-4, synthesized by osteoblasts, is one of the most potent inducers of bone formation, promoting osteoblast differentiation[38]. BMP-7 has been shown to stimulate osteoblastic differentiation in rat calvarial, mouse, and human bone marrow stromal cells, along with increased alkaline phosphatase activity, collagen production, and osteocalcin synthesis[39]. Samara et al. measured BMP levels in femoral heads obtained from patients undergoing total hip arthroplasty due to ONFH head and found increased BMP-4 levels in necrotic areas, whereas BMP-7 levels were significantly reduced[40]. Similarly, Zhang et al., in a study investigating the effects of platelet-rich plasma and tricalcium phosphate combination therapy on ONFH following femoral neck fractures in rabbits, reported higher BMP-7 levels in the treatment group compared to the control group[41]. In our study, no statistically significant differences were observed between groups in terms of BMP-4 levels. However, BMP-7 levels were found to be higher in the Ap-13-treated ONFH group, consistent with findings from the literature.

Accumulating evidence indicates that steroid-induced ONFH is driven, at least in part, by hyperactive osteoclasts amplified under oxidative stress[42–44]. In human necrotic femoral heads and rat SONFH models, osteoclast markers (TRAP, CTSK) and the RANKL/OPG axis are up-regulated in parallel with diminished antioxidant enzymes and higher ROS signals, supporting a ROS-osteoclast feed-forward loop in early progression[42]. Consistently, pharmacologic anti-osteoclast strategies mitigate disease severity: in a recent in-vivo SONFH study, the natural inhibitor cycloastragenol reduced necrotic lesion size, improved trabecular parameters and blood supply, lowered RANKL/OPG ratio, down-regulated TRAP/CTSK/MMP9, and decreased empty lacunae[43]. Inflammation also feeds osteoclastogenesis via NF-κB/AP-1 signaling; modulation of these pathways (e.g., GILZ-linked anti-inflammatory signaling) can blunt downstream effector responses relevant to bone resorption[44]. In our study, Ap-13 reduced oxidative stress (lower serum MDA, trend to higher GSH), attenuated apoptosis (reversal of caspase-3 increases), enhanced endothelial VEGF immunoreactivity, and improved trabecular architecture. These effects map onto the above mechanisms in two ways: (i) by limiting ROS, Ap-13 May secondarily restrain osteoclast hyperactivation; and (ii) by improving microvascular integrity, it may reduce the ischemic triggers that sustain resorption. Although we observed normalization of OPG levels with Ap-13, the net RANKL/OPG balance—a key determinant of osteoclast activity—was not directly measured and merits dedicated follow-up. Overall, our data align with the concept that antioxidant and vasculoprotective interventions (such as Ap-13) may indirectly temper inflammation- and ROS-driven osteoclast activity, thereby slowing SONFH progression.

Our study has some limitations. To adhere to the 3 R principle commonly accepted in scientific studies involving animals, a smaller number of animals were used, and less stimulation was applied under appropriate conditions[45]. Due to these limitations, the intraperitoneal and intramuscular injections administered during the first week and the intraperitoneal applications throughout the study caused sufficient stress in the rats, leading to biochemical analyses being conducted at the end of the study. Another limitation of our study is the use of a single dose of Ap-13. Further research is needed to explore the dosing effects and determine the optimal dose for reducing the incidence of steroid-induced osteonecrosis. Additionally, the 4-week observation period designed in our study may be shortened to assess

the short-term efficacy of Ap-13 treatment. Therefore, future studies should address these issues in greater detail. Another limitation of our study is that we did not evaluate the endogenous expression levels of Apelin-13 in normal or osteonecrotic femoral heads, nor did we perform gene knockdown experiments. Similar to previous studies focusing on the therapeutic effects of Apelin-13 without assessing its local expression[46], future research incorporating expression analyses and loss-of-function approaches will be essential to elucidate the precise role of Apelin-13 in SONFH pathogenesis.

Taken together, our findings support the therapeutic potential of Apelin-13 (Ap-13), a potent antioxidant peptide, in protecting against steroid-induced osteonecrosis of the femoral head. Ap-13 was shown to attenuate oxidative stress, reduce apoptosis, enhance vascularization, and preserve trabecular bone architecture in a rat model of SONFH. These multifactorial effects suggest that Ap-13 May intervene at several critical points in the pathogenesis of osteonecrosis. Although some parameters showed modest numerical differences between groups, statistically significant outcomes indicate consistent biological effects. With larger sample sizes, longer follow-up periods, and dose-optimization studies, the protective efficacy of Ap-13 May become even more evident, potentially offering a promising noninvasive strategy for the prevention and management of early-stage osteonecrosis.

Disclosure statement

No potential conflict of interest was reported by the author(s).

Ethical review committee Statement

The animal experiments in this study were approved by the local ethics committee; approval was obtained from the Experimental Research and Skill Development Center (BADABEM) of the Istanbul Bağcılar Health Application and Research Center, Health Sciences University (Meeting date: 23 December 2022, Meeting No: 2022/52, Project No: 2022–14).

Throughout the study, it was conducted in compliance with the European Convention for the Protection of Vertebrate Animals Used for Experimental and Other Scientific Purposes (ETS-123) at BADABEM. During the planning of the study, standard procedures related to preclinical animal studies and research were designed and implemented.

Funding

The author(s) reported there is no funding associated with the work featured in this article.

ORCID

Ozancan Biçer http://orcid.org/0000-0002-6080-177X
Ozan Beytemur http://orcid.org/0000-0002-9608-7280
Mustafa Fatih Daşci http://orcid.org/0000-0002-2443-4802
Muhammed Uslu http://orcid.org/0000-0002-1810-2713
Yiğit Güleryüz http://orcid.org/0000-0002-9220-9578
Yiğit Önaloğlu http://orcid.org/0000-0002-3893-797X
Emin Can Balci http://orcid.org/0000-0002-1565-9620
Büşra Yaprak Bayrak http://orcid.org/0000-0002-0537-3127

References

1. Petek D, Hannouche D, Suva D. Osteonecrosis of the femoral head: pathophysiology and current concepts of treatment. EFORT Open Rev. 2019;4(3):85–97. doi:10.1302/2058-5241.4.180036.
2. Mont MA, Salem HS, Piuzzi NS, Goodman SB, Jones LC. Nontraumatic osteonecrosis of the femoral head: where do we stand today? J Bone Joint Surg Am. 2020;102(12):1084–1099. doi:10.2106/JBJS.19.01271.
3. Abani O, Abbas A, Abbas F, Abbas J, Abbas K, Abbas M, Abbasi S, Abbass H, Abbott A, Abbott A, et al. Higher dose corticosteroids in patients admitted to hospital with COVID-19 who are hypoxic but not requiring ventilatory support (recovery): a randomised, controlled, open-label, platform trial. Lancet Lond Engl. 2023;401(10387):1499–1507. doi:10.1016/S0140-6736(23)00510-X.
4. George G, Lane JM. Osteonecrosis of the femoral head. JAAOS Glob Res Rev. 2022;6(5):e21.00176. doi:10.5435/JAAOSGlobal-D-21-00176.
5. Salman LA, Hantouly AT, Khatkar H, Al-Ani A, Abudalou A, Al-Juboori M, Ahmed G. The outcomes of total hip replacement in osteonecrosis versus osteoarthritis: a systematic review and meta-analysis. Int Orthop. 2023;47(12):3043–3052. doi:10.1007/s00264-023-05761-6.
6. Wang W, Jiang H, Yu J, Lou C, Lin J. Astaxanthin-mediated Nrf2 activation ameliorates glucocorticoid-induced oxidative stress and mitochondrial dysfunction and impaired bone formation of glucocorticoid-induced osteonecrosis of the femoral head in rats. J Orthop Surg. 2024;19(1):294. doi:10.1186/s13018-024-04775-z.
7. Gong G, Wan W, Liu X, Yin J. Apelin-13, a regulator of autophagy, apoptosis and inflammation in multifaceted bone protection. Int Immunopharmacol. 2023;117:109991. doi:10.1016/j.intimp.2023.109991.
8. Xu J, Gong H, Lu S, Deasey MJ, Cui Q. Animal models of steroid-induced osteonecrosis of the femoral head—a comprehensive research review up to 2018. Int Orthop. 2018;42(7):1729–1737. doi:10.1007/s00264-018-3956-1.
9. Costa FWG, de Brito GA, Pessoa RMA, ve Studart-Soares EC. Histomorphometric assessment of bone necrosis produced by two cryosurgery protocols using liquid nitrogen: an experimental study on rat femurs. J Appl Oral Sci Rev. 2011;19(6):604–609. doi:10.1590/s1678-77572011000600010.

10. Chen S, Li J, Peng H, Zhou J, Fang H. Administration of erythropoietin exerts protective effects against glucocorticoid-induced osteonecrosis of the femoral head in rats. Int J Mol Med. 2014;33(4):840–848. doi:10.3892/ijmm.2014.1644.
11. Zhao D, Zhang F, Wang B, Liu B, Li L, Kim S-Y, Goodman SB, Hernigou P, Cui Q, Lineaweaver WC, et al. Guidelines for clinical diagnosis and treatment of osteonecrosis of the femoral head in adults (2019 version). J Orthop Translat. 2020;21:100–110. doi:10.1016/j.jot.2019.12.004.
12. Boucher J, Masri B, Daviaud D, Gesta S, Guigné C, Mazzucotelli A, Tack I, Knibiehler B, Carpéné C, Audigier Y. Apelin, a newly identified adipokine up-regulated by insulin and obesity. Endocrinology. 2005;146(4):1764–1771. doi:10.1210/en.2004-1427.
13. Fan Z, Bai S, Xu Q, Li Z, Cui W, Li H, Zhang H-F. Oxidative stress induced osteocyte apoptosis in steroid-induced femoral head necrosis. Orthop Surg. 2021;13(7):2145–2152. doi:10.1111/os.13127.
14. Tao SC, Yuan T, Rui BY, Zhu ZZ, Guo SC, Zhang CQ. Exosomes derived from human platelet-rich plasma prevent apoptosis induced by glucocorticoid-associated endoplasmic reticulum stress in rat osteonecrosis of the femoral head via the Akt/Bad/Bcl-2 signal pathway. Theranostics. 2017;7(3):733–750. doi:10.7150/thno.17450.
15. Komurcu E. Preventive effects of coenzyme Q10 (CoQ10) on steroid-induced osteonecrosis in rats. Acta Orthop Traumatol Turc. 2014;2(2):217–222. doi:10.3944/AOTT.2014.13.0150.
16. Ichiseki T, Ueda Y, Katsuda S, Kitamura K, Kaneuji A, Matsumoto T. Oxidative stress by glutathione depletion induces osteonecrosis in rats. Rheumatology. 2006;45(3):287–290. doi:10.1093/rheumatology/kei149.
17. Deng G, Dai C, Chen J, Ji A, Zhao J, Zhai Y, Kang Y, Liu X, Wang Y, Wang Q. Porous Se@SiO2 nanocomposites protect the femoral head from methylprednisolone-induced osteonecrosis. Int J Nanomed, C. 2018;13:ss. 1809–1818. doi:10.2147/IJN.S159776.
18. Piatek S, Adolf D, Wex T, Halangk W, Klose S, Westphal S, Winckler S. Multiparameter analysis of serum levels of C-telopeptide crosslaps, bone-specific alkaline phosphatase, cathepsin K, osteoprotegerin and receptor activator of nuclear factor κB ligand in the diagnosis of osteoporosis. Maturitas. 2013;74(4):363–368. doi:10.1016/j.maturitas.2013.01.005.
19. Ye J, Wei D, Peng L, Chang T. Ginsenoside Rb1 prevents steroid-induced avascular necrosis of the femoral head through the bone morphogenetic protein-2 and vascular endothelial growth factor pathway. Mol Med Rep. 2019;20(4):3175–3181.
20. Zhou D, Chen YX, Yin JH, Tao SC, Guo SC, Wei ZY, Feng Y, Zhang C. Valproic acid prevents glucocorticoid-induced osteonecrosis of the femoral head of rats. Int J Mol Med. 2018;41(6):3433–3447. doi:10.3892/ijmm.2018.3534.
21. Yasuda H. Discovery of the RANKL/RANK/OPG system. J Bone Min Metab. 2021;39(1):2–11. doi:10.1007/s00774-020-01175-1.
22. Peng WX, Ye C, Dong WT, Yang LL, Wang CQ, Wei ZA, Li V, Deng J, Zhang J. MicroRNA-34a alleviates steroid-induced avascular necrosis of femoral head by targeting Tgif2 through OPG/RANK/RANKL signaling pathway. Exp Biol Med. 2017;242(12):1234–1243. doi:10.1177/1535370217703975.
23. Rs W, Rw N, Sc M. Apoptosis of osteocytes in glucocorticoid-induced osteonecrosis of the hip. J Clin Endocrinol Metab. 2000;85(8):2907–2912. doi:10.1210/jc.85.8.2907.
24. Weinstein SL. Bristol-myers Squibb/Zimmer award for distinguished achievement in orthopaedic research: long-term follow-up of pediatric orthopaedic conditions: natural history and outcomes of treatment. JBJS. 2000;82(7):980.
25. Sato AY, Tu X, McAndrews KA, Plotkin LI, Bellido T. Prevention of glucocorticoid induced-apoptosis of osteoblasts and osteocytes by protecting against endoplasmic reticulum (ER) stress in vitro and in vivo in female mice. Bone. 2015;60. doi:10.1016/j.bone.2014.12.012.
26. Sun Y, Liang M, Xing Y, Duan Y, Zhang S, Deng B. Cyasterone has a protective effect on steroid-induced osteonecrosis of the femoral head. PLOS ONE. 2023;18(10):e0293530. doi:10.1371/journal.pone.0293530.
27. Feng X, Liu Z, Su Y, Lian H, Gao Y, Zhao J, Xu J, Liu Q, Song F. Tussilagone inhibits osteoclastogenesis by modulating mitochondrial function and ros production involved Nrf2 activation. Biochemical Pharmacol. 2023 Dec 1;218:115895. doi:10.1016/j.bcp.2023.115895.
28. Jin C, Yu XB, Yang J, Lin Z, Ma RX, Lin BH, Zhang HJ, Dai ZH, Xue K, Xie CL, et al. Corynoline suppresses osteoclastogenesis and attenuates ros activities by regulating NF-κB/MAPKs and Nrf2 signaling pathways. J Agr Food Chem. 2024 Mar 29;72(14):8149–8166. doi:10.1021/acs.jafc.3c07088.
29. Chen Z, Yao H, Encarnacion AM, Jeong J, Choi Y, Park S, Lee S, Lee T. Novel inhibitor of Keap1-Nrf2 protein–protein interaction attenuates osteoclastogenesis in vitro and prevents OVX-Induced bone loss in vivo. Antioxidants. 2024 Jul 15;13(7):850. doi:10.3390/antiox13070850.
30. Xu Y, Song D, Su Y, Chen J, Wu L, Lian H, Hai N, Jiang J, Zhao J, Xu J, et al. Pharmacology-based molecular docking of 4-methylcatechol and its role in RANKL-mediated ROS/Keap1/Nrf2 signalling axis and osteoclastogenesis. Biomed Pharmacother. 2023 Mar 1;159:114101.
31. Wei L, Chen W, Huang L, Wang H, Su Y, Liang J, Lian H, Xu J, Zhao J, Liu Q. Alpinetin ameliorates bone loss in LPS-induced inflammation osteolysis via ros mediated P38/PI3K signaling pathway. Pharmacol Res. 2022 Oct 1;184:106400. doi:10.1016/j.phrs.2022.106400.
32. Zhao Y, Li D, Duan DP, Song QC. The effect of endostatin on angiogenesis and osteogenesis of steroid-induced osteonecrosis of the femoral head in a rabbit model. Acta Orthop Traumatol Turc. 2022;56(3):178–186. doi:10.5152/j.aott.2022.21248.
33. Tabouret T, Gregory T, Dhooge M, Brezault C, Mir O, Dréanic J, Chaussade S, Coriat R. Long term exposure

to antiangiogenic therapy, bevacizumab, induces osteonecrosis. Invest New Drugs. 2015;33 (5):1144–1147. doi:10.1007/s10637-015-0283-x.
34. Song Q, Ni J, Jiang H, Shi Z. Sildenafil improves blood perfusion in steroid-induced avascular necrosis of femoral head in rabbits via a protein kinase G-dependent mechanism. Acta Orthop Traumatol Turc. 2017;51(5):398–403. doi:10.1016/j.aott.2017.07.002.
35. Özmen E, İzol Özmen H, Atasoy S, Dursun M, Bilgiç B, Salduz A. The effects of prophylactic tadalafil use on VEGF expression in the rabbit model of steroid-induced femoral head avascular necrosis. Acta Orthop Traumatol Turc. 2023 Sep;57(5):237–242. doi:10.5152/j.aott.2023.22188.
36. Wang A, Ren M, Wang J. The pathogenesis of steroid-induced osteonecrosis of the femoral head: a systematic review of the literature. Gene. 2018;671:103–109. doi:10.1016/j.gene.2018.05.091.
37. Wang XY, Ma TL, Chen KN, Pang ZY, Wang H, Huang JM, Qi G-B, Wang C-Z, Jiang Z-X, Gong L-J, et al. Accumulation of LDL/ox-LDL in the necrotic region participates in osteonecrosis of the femoral head: a pathological and in vitro study. Lipids Health Dis. 2021;20(1):167. doi:10.1186/s12944-021-01601-x.
38. Chang SF, Chang TK, Peng HH, Yeh YT, Lee DY, Yeh CR, Cheng V, Chang CA, Chiu J-J. BMP-4 induction of arrest and differentiation of osteoblast-like cells via p21CIP1 and p27KIP1 regulation. Mol Endocrinol. 2009;23(11):1827–1838. doi:10.1210/me.2009-0143.
39. Sampath TK, Maliakal JC, Hauschka PV, Jones WK, Sasak H, Tucker RF, White KH, Coughlin JE, Tucker MM, Pang RH. Recombinant human osteogenic protein-1 (hOP-1) induces new bone formation in vivo with a specific activity comparable with natural bovine osteogenic protein and stimulates osteoblast proliferation and differentiation in vitro. J Biol Chem. 1992;267 (28):20352–20362. doi:10.1016/S0021-9258(19)88709-4.
40. Samara S, Dailiana Z, Varitimidis S, Chassanidis C, Koromila T, Malizos KN. Bone morphogenetic proteins (BMPs) expression in the femoral heads of patients with avascular necrosis. Mol Biol Rep. 2013;40(7):4465–4472. doi:10.1007/s11033-013-2538-y.
41. Zhang XL, Wang YM, Chu K, Wang ZH, Liu YH, Jiang LH. The application of PRP combined with TCP in repairing avascular necrosis of the femoral head after femoral neck fracture in rabbit. Eur Rev Med Pharmacol Sci. 2018;22(4):903–909. doi:10.26355/eurrev_201802_14368.
42. Chen K, Liu Y, He J, Pavlos N, Wang C, Kenny J, Yuan J, Zhang Q, Xu J, He W. Steroid-induced osteonecrosis of the femoral head reveals enhanced reactive oxygen species and hyperactive osteoclasts. Int J Biol Sci. 2020 Apr 6;16(11):1888. doi:10.7150/ijbs.40917.
43. Wang G, Ma C, Mo L, Chen J, Yuan J, Xu J, He W. Cycloastragenol prevents bone loss via inhibiting osteoclast activity in glucocorticoid-induced osteonecrosis of the femoral head: an in vivo study. J Orthop Transl. 2024 Mar 1;45:178–187. doi:10.1016/j.jot.2024.01.009.
44. Ngo D, Beaulieu E, Gu R, Leaney A, Santos L, Fan H, Yang Y, Kao W, Xu J, Escriou V, et al. Divergent effects of endogenous and exogenous glucocorticoid-induced leucine zipper in animal models of inflammation and arthritis. Arthritis Rheum. 2013 May;65(5):1203–1212. doi:10.1002/art.37858.
45. Hubrecht RC, Carter E. The 3Rs and humane experimental technique: implementing change. Anim Open Access J MDPI. 2019;9(10):754. doi:10.3390/ani9100754.
46. Hang K, Ye C, Xu J, Chen E, Wang C, Zhang W, Ni L, Kuang Z, Ying L, Xue D, et al. Apelin enhances the osteogenic differentiation of human bone marrow mesenchymal stem cells partly through Wnt/β-catenin signaling pathway. STEM Cell Res Ther. 2019;10 (1):189. doi:10.1186/s13287-019-1286-x.